

IMAGE DATA ANALYSIS (6CFU)

MODULE OF
REMOTE SENSING
(9 CFU)

A.Y. 2022/23
MASTER OF SCIENCE IN COMMUNICATION TECHNOLOGIES AND MULTIMEDIA
MASTER OF SCIENCE IN COMPUTER SCIENCE, LM INGEGNERIA INFORMATICA

PROF. ALBERTO SIGNORONI

ERROR CORRECTION AND REGISTRATION OF IMAGE DATA

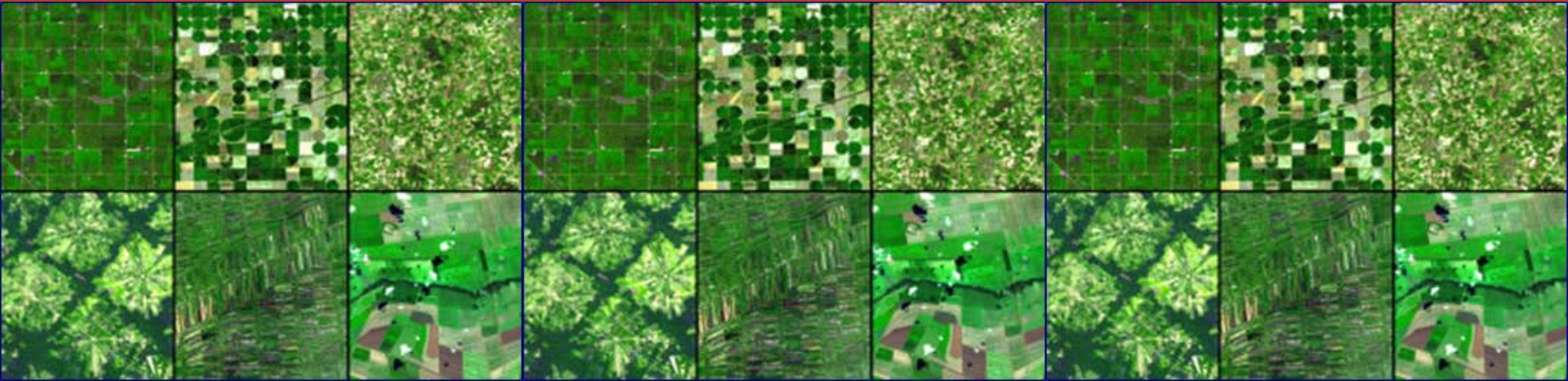


Image data acquisition

Image acquisition systems



Digital imaging
inspection,
detection,
quantification,
recognition
quality control,
design,

...

3D imaging

- Internal (CT)
- External (3D scan)

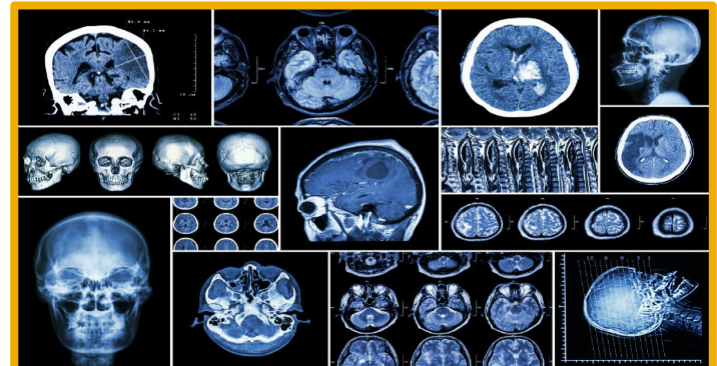
(hyper)spectral imaging

Applications

Remote sensing



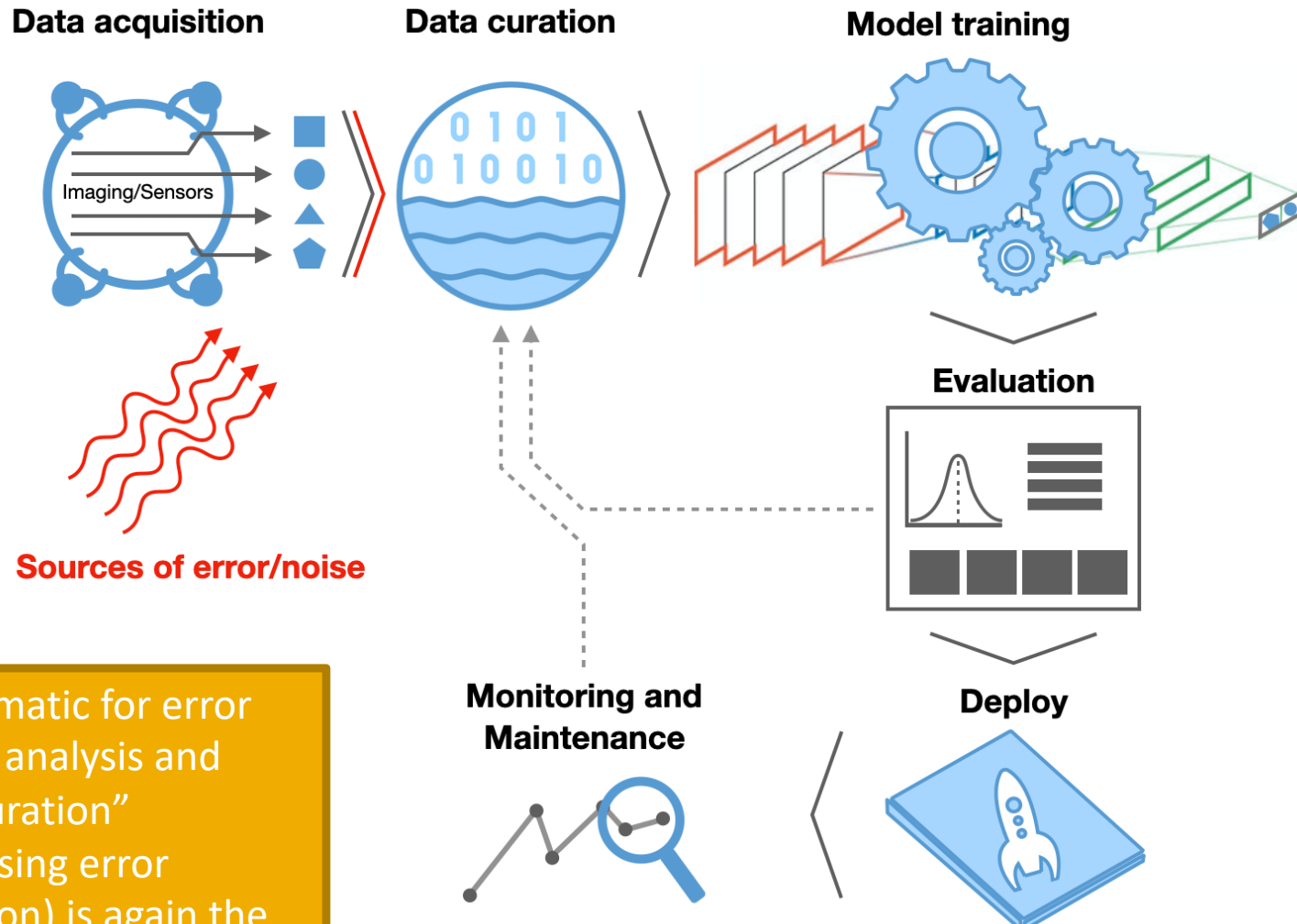
Medical imaging



Industrial imaging



Sources of error in the (data-driven) image analysis pipeline



Paradigmatic for error sources analysis and data “curation” (comprising error correction) is again the case of **Remote Sensing applications**

Sources of error in Remote Sensing data

- When image data is recorded by sensors on satellites and aircraft it can contain errors in geometry and in the measured brightness values of the pixels
 - *this can happen also for many other professional fields of application at various scales: industrial, biomedical, cultural heritage, submarine, microscopy,...*
- Brightness errors are referred to as **radiometric errors** and can result
 - from the **instrumentation** used to record the data,
 - from the **wavelength dependence** of solar radiation and
 - from the effect of the **atmosphere**.
- Image **geometry errors** can arise in many ways.
 - The **relative motions** of the platform, its scanners and the earth, for example, can lead to errors of a skewing nature in an image product.
 - **Non-idealities in the sensors** themselves, the **curvature of the earth** and **uncontrolled position and altitude variations** of the remote sensing platform can all lead to geometric errors of varying degrees of severity.
- For many applications only the major sources of error will require compensation whereas in others more precise correction will be necessary.

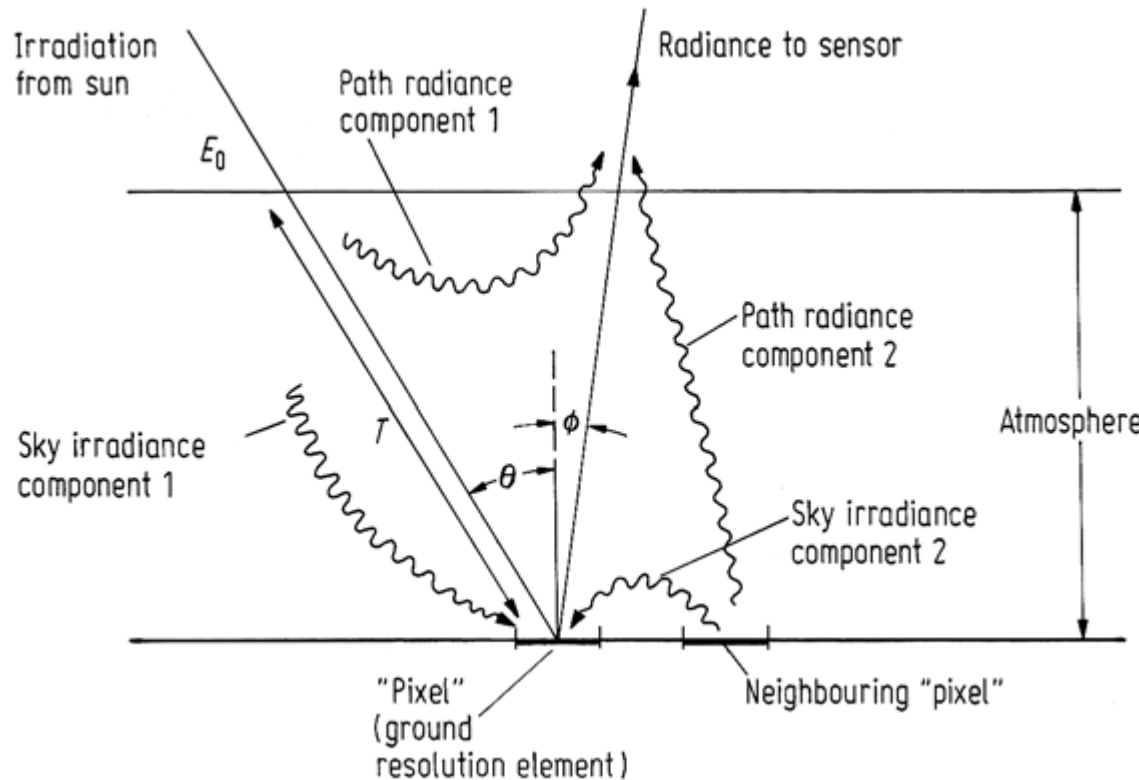
SOURCES OF RADIOMETRIC DISTORTION IN REMOTE SENSING DATA

Types of radiometric distortion

- Mechanisms that affect the measured brightness values of the pixels in an image can lead to two broad types of radiometric distortion.
 1. **Intra-band:** the **relative distribution of brightness** over an image in a given band can be different to that in the **ground scene**.
 2. **Inter-band:** the **relative brightness of a single pixel from band to band** can be distorted compared with the **spectral reflectance character of the corresponding region on the ground**.
- Both types can result from the presence of the atmosphere as a transmission medium through which radiation must travel from its source to the sensors, and can be a result also of instrumentation effects.

The Effect of the Atmosphere on Radiation

- The figure depicts the **effect the atmosphere has on the measured brightness value of a single pixel for a passive remote sensing system** in which the sun is the source of energy, as in the visible and reflective infrared regions.
 - In the absence of an atmosphere the signal measured by the sensor will be a function simply of the level of energy from the sun, actually incident on the pixel, and the reflectance properties of the pixel itself.
 - However, the presence of the atmosphere can modify the situation significantly



Radiometric quantity definitions

- Imagine the sun as a source of energy emitting at a given rate of Joules per second, or Watts.
 - This energy radiates through space *isotropically* in an inverse square law fashion so that at a given distance the sun's emission can be measured as Watts per square meter (given as the power emitted divided by the surface area of a sphere at that distance).
 - This power density is called **irradiance**, a property that can be used to describe the strength of any emitter of electromagnetic energy (Wm^{-2}).
- We can measure a level of solar irradiance at the earth's surface. If the surface is perfectly diffuse then this amount is scattered uniformly into the upper hemisphere.
 - The amount of power density scattered in a particular direction is defined by its density per solid angle, since equal amounts are scattered into equal cones of solid angle.
 - This quantity is called **radiance** and has units of Watts per square meter per steradian ($\text{Wm}^{-2}\text{sr}^{-1}$).
- The emission of energy by bodies such as the sun is **wavelength dependent**, as already seen (black body radiation)
 - The term **spectral irradiance** is used to describe how much power density is available incrementally across the wavelength range.
 - Spectral irradiance is typically measured in $\text{Wm}^{-2}\mu\text{m}^{-1}$.

Radiometric quantity definitions

As an illustration of how these quantities might be used suppose, in the absence of atmosphere, the solar spectral irradiance at the earth is E_λ . If the solar zenith angle (measured from the normal to the surface) is θ as shown in Figure then the spectral irradiance (spectral power density) on the earth's surface is $E_\lambda \cos \theta$. This gives an available irradiance between wavelengths λ_1 and λ_2 of

$$E_{os} = \int_{\lambda_1}^{\lambda_2} E_\lambda \cos \theta d\lambda. \quad \text{Wm}^{-2}$$

In remote sensing the wavebands used ($\Delta\lambda = \lambda_2 - \lambda_1$) are frequently narrow enough to assume

$$E_{os} = E_{\Delta\lambda} \cos \theta \Delta\lambda \quad \text{Wm}^{-2} \quad (2.1)$$

where $E_{\Delta\lambda}$ is the average spectral irradiance in the band $\Delta\lambda$.

Radiometric quantity definitions

Suppose the surface has a reflectance R . This describes what proportion of the incident energy is reflected. If the surface is diffuse then the radiance scattered into the upper hemisphere and available for measurement is

$$L = E_{\Delta\lambda} \cos \theta \Delta\lambda R / \pi \quad \text{Wm}^{-2}\text{sr}^{-1} \quad (2.2)$$

where the divisor π accounts for the upper hemisphere of solid angle. Knowing L it is possible to determine the power detected by a sensor, and the digital count value (or grey level) given in the digital data product from a particular sensor which is directly related to the radiance of the scene. If we call the digital value (between 0 and 255 for example) C , then the measured radiance of a particular pixel is

$$L = Ck + L_{min} \quad \text{Wm}^{-2}\text{sr}^{-1} \quad (2.3)$$

where $k = (L_{max} - L_{min})/C_{max}$ in which L_{max} and L_{min} are the maximum and minimum measurable radiances of the sensor. These are usually available from the sensor manufacturer or operator.

Equation (2.2) relates to the ideal case of no atmosphere. When an atmosphere is present there are several mechanism that must be taken into account that modify (2.2). These are a result of scattering and absorption by the particles in the atmosphere.

See for example <https://www.youtube.com/watch?v=gLfYTP4F23g> to dig a bit more into radiometric quantities.

Absorption and scattering by the atmosphere

- **Absorption by atmospheric molecules** is a selective process that converts incoming energy into heat.
 - In particular, molecules of oxygen, carbon dioxide (CO_2), ozone (O_3), and water attenuate the radiation *very strongly in certain wavebands*.
 - Sensors commonly used in solid earth and ocean remote sensing are usually designed to *operate away* from these regions so that the effects are small.
- **Scattering by atmospheric particles** is then the dominant mechanism that leads to radiometric distortion in image data (apart from sensor effects).
- There are two broadly identified scattering mechanisms.
 1. The first is scattering by the air molecules themselves. This is called **Rayleigh scattering** and is an *inverse fourth power function of the wavelength used*.
 2. The other is called **aerosol or Mie scattering** and is a result of scattering of the radiation from *larger particles such as those associated with smoke, haze and fumes (e.g. from cars)*. These particulates are of the order of *one tenth to ten wavelengths*.
- Mie scattering is also wavelength dependent, although not as strongly as Rayleigh scattering. When the atmospheric particulates become much larger than a wavelength, such as those common in fogs, clouds and dust, the wavelength dependence disappears.

Absorption and scattering by the atmosphere

- In a clear ideal atmosphere Rayleigh scattering is the only mechanism present.
 - It accounts, for example, for the *blueness of the sky*. Because the shorter (blue) wavelengths are scattered more than the longer (red) wavelengths we are more likely to see blue when looking in any direction in the sky.
 - Likewise the *reddish appearance of sunset* is also caused by Rayleigh scattering. This is a result of the long atmospheric path the radiation has to follow at sunset during which most short wavelength radiation is scattered away from direct line of sight by comparison to the longer wavelengths.
- In contrast to Rayleigh scattering, fogs and clouds appear white or bluish-white owing to the (near) non-selective scattering caused by the larger particles.

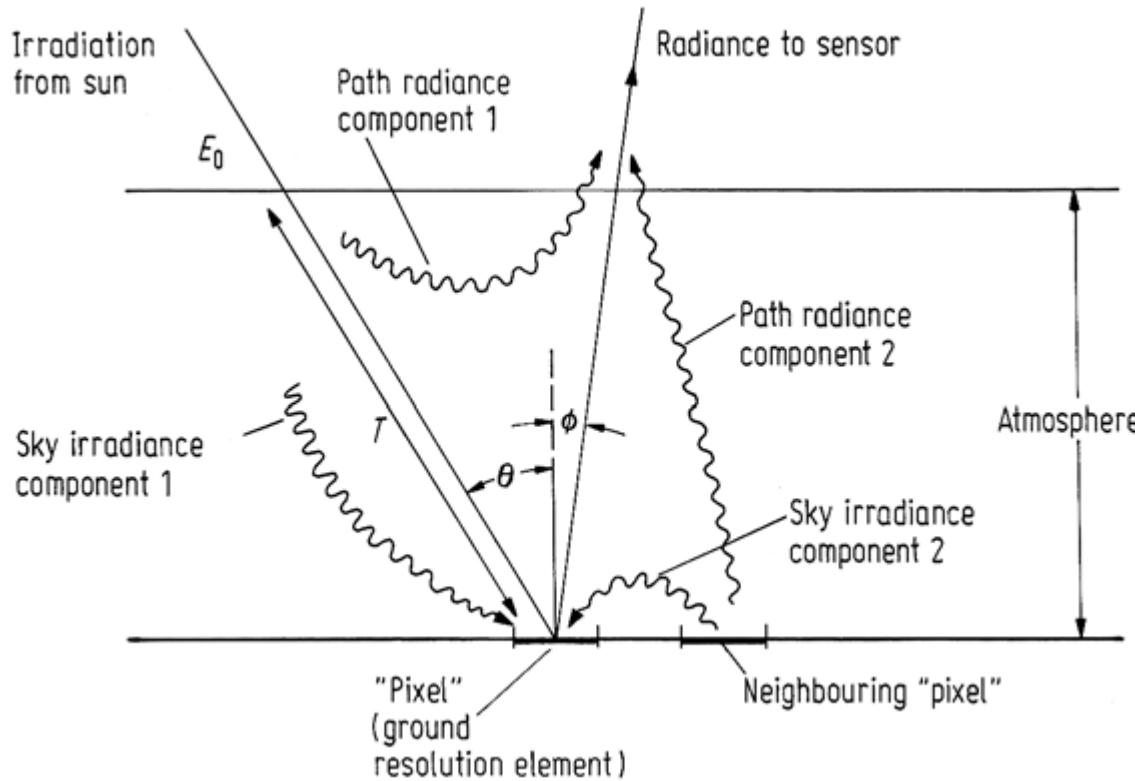


We are now in the position to “*appreciate*” the effect of the atmosphere on the radiation that ultimately reaches a sensor.



(back to) The Effect of the Atmosphere on Radiation

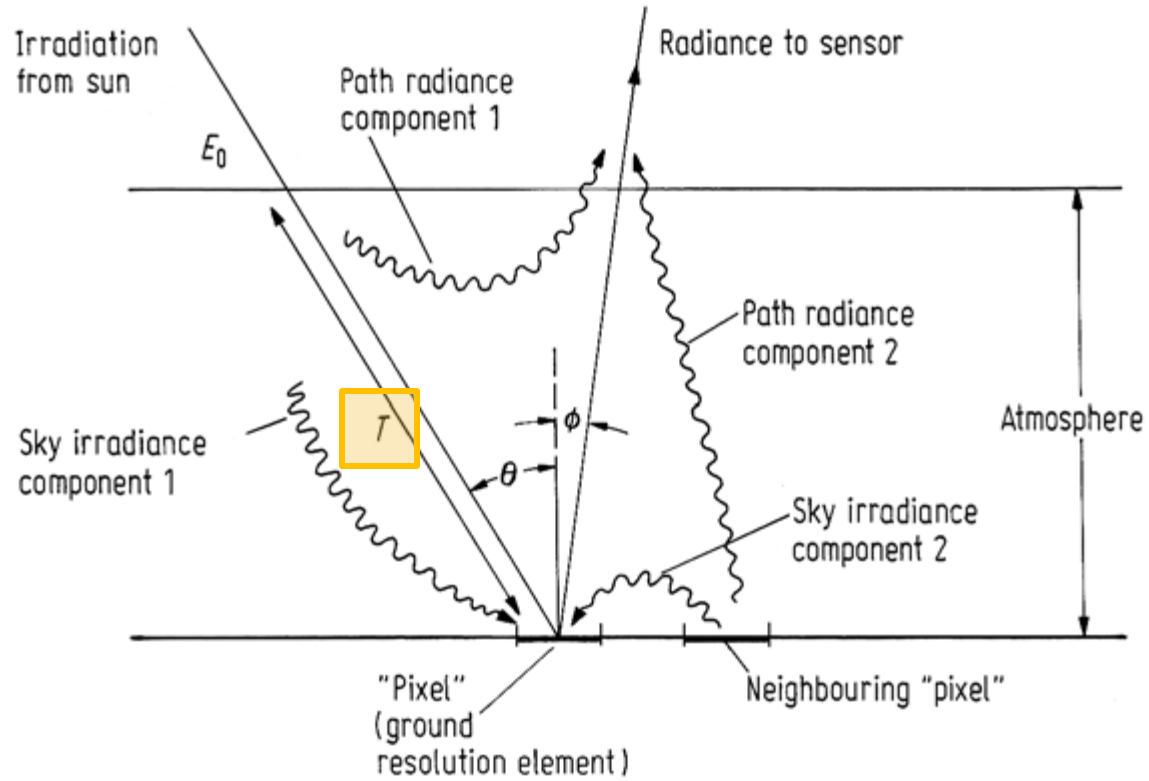
- The figure depicts the **effect the atmosphere has on the measured brightness value of a single pixel for a passive remote sensing system** in which the sun is the source of energy, as in the visible and reflective infrared regions.
 - In the absence of an atmosphere the signal measured by the sensor will be a function simply of the level of energy from the sun, actually incident on the pixel, and the reflectance properties of the pixel itself.
 - However, the presence of the atmosphere can modify the situation significantly



The Effect of the Atmosphere on Radiation (cont.)

□ Transmittance

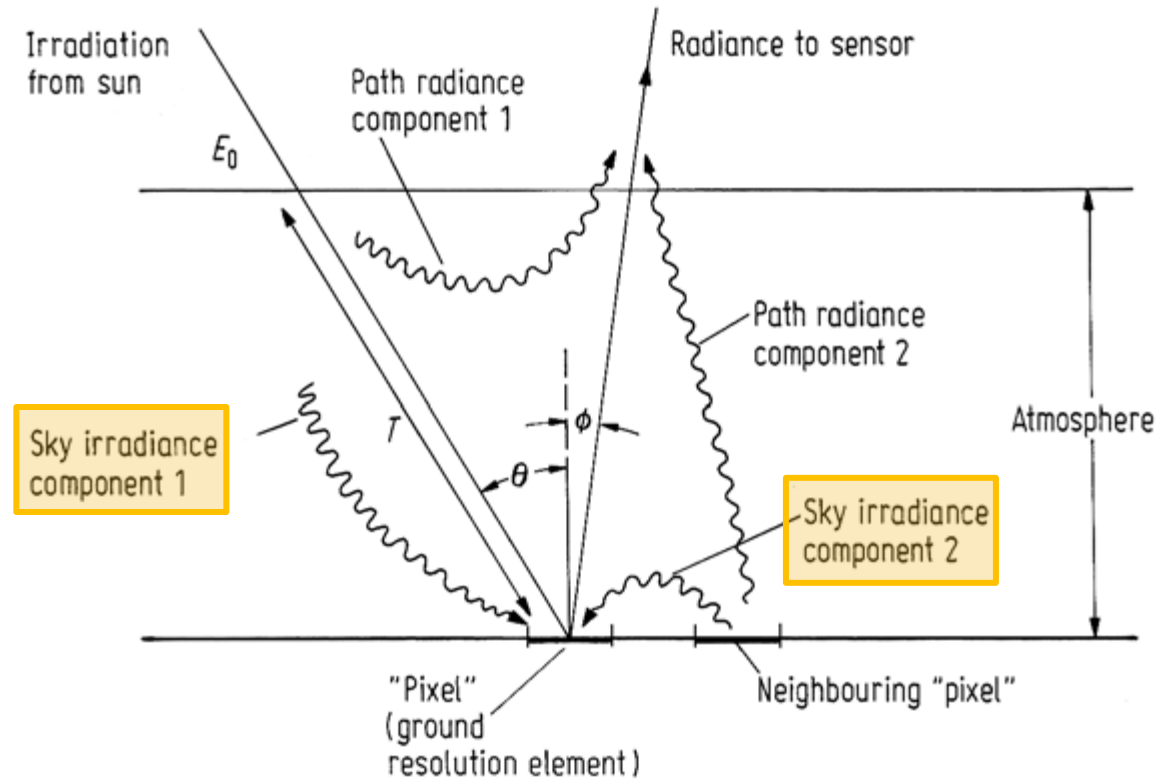
- In the absence of atmosphere transmittance is 100%. However, because of scattering and absorption not all of the available solar irradiance reaches the ground. The amount that does, relative to that for no atmosphere, is called the *transmittance*.
- Let this be called T_θ , the subscript indicating its dependence on the zenith angle of the source because of the longer path length through the atmosphere. In a similar way there is an atmospheric transmittance T_ϕ to be taken into account between the point of reflection and the sensor.



The Effect of the Atmosphere on Radiation (cont.)

□ *Sky irradiance*

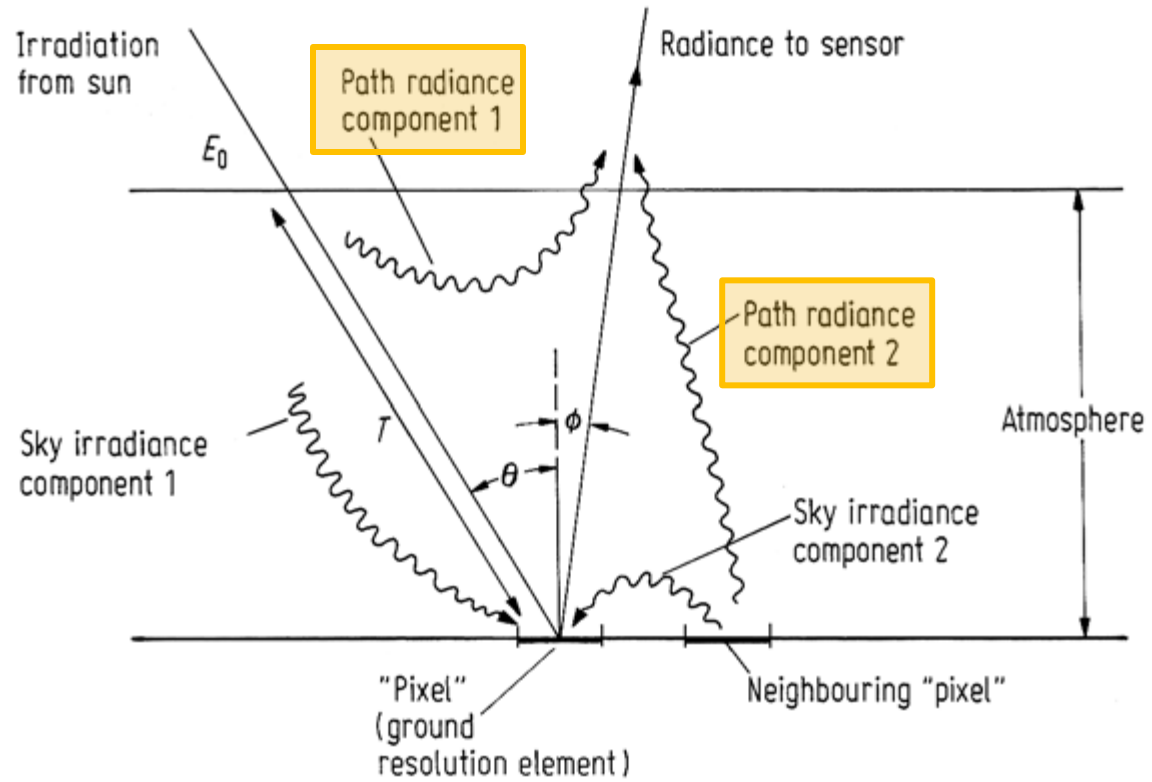
- Because the radiation is scattered on its travel down through the atmosphere a particular pixel will be irradiated both by energy on the direct path and also by energy scattered from atmospheric constituents. This is the sky irradiance component 1 in Figure, which path is undefined and in fact diffuse.
- A pixel can also receive some energy that has been reflected from surrounding pixels and then, by atmospheric scattering, is again directed downwards. This is the sky irradiance component 2 in Figure.
- We will call the sky irradiance at the pixel E_D .



The Effect of the Atmosphere on Radiation (cont.)

□ Path radiance

- Again because of scattering alone, radiation can reach the sensor from adjacent pixels and also via diffuse scattering of the incoming radiation that is actually scattered towards the sensor by the atmospheric constituents before it reaches the ground. These two components are referred to as path radiance and denoted L_p .



Radiometric quantity definitions

Having defined these effects we are now in the position to determine how the radiance measured by the sensor is affected by the presence of the atmosphere. First the total irradiance at the earth's surface now becomes, instead of (2.1)

$$E_G = E_{\Delta\lambda} T_\theta \cos \theta \Delta\lambda + E_D \quad \text{Wm}^{-2}$$

$$E_{os} = E_{\Delta\lambda} \cos \theta \Delta\lambda$$

where, for simplicity, it has been assumed that the diffuse sky irradiance is not a function of wavelength (in the waveband of interest). The radiance therefore due to this global irradiance of the pixel becomes

$$L_T = \frac{R}{\pi} \{E_{\Delta\lambda} T_\theta \cos \theta \Delta\lambda + E_D\} \quad \text{Wm}^{-2} \text{sr}^{-1}$$

Above the atmosphere the total radiance available to the sensor then becomes

$$L_s = \frac{RT_\phi}{\pi} \{E_{\Delta\lambda} T_\theta \cos \theta \Delta\lambda + E_D\} + L_p \quad \text{Wm}^{-2} \text{sr}^{-1} \quad (2.4)$$

It is this quantity therefore that should be used in (2.3) to relate the digital count value to measured radiance.

$$L = Ck + L_{min}$$

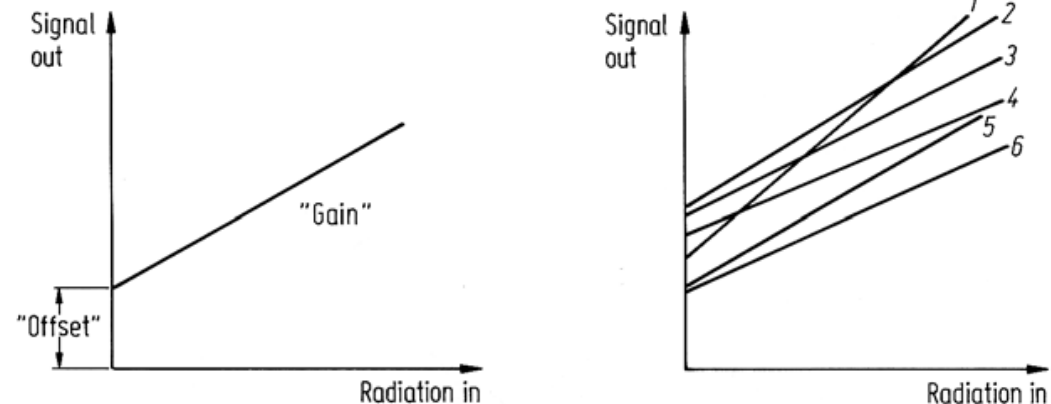
Atmospheric Effects on Remote Sensing Imagery

- A result of the scattering caused by the atmosphere is that ***fine detail in image data will be obscured***. Consequently, it is important in applications where one is dependent upon the limit of sensor resolution available, such as in *urban studies*, to take steps to correct for atmospheric effects.
- It is important also to consider carefully the effects of the atmosphere on remote sensing systems with wide fields of view in which there will be an appreciable ***difference in atmospheric path length*** between nadir and the extremities of the swath.
- Finally, and perhaps most importantly, because both Rayleigh and Mie scattering are wavelength dependent, ***the effects of the atmosphere will be different in the different wavebands*** of a given sensor system.
 - In the case of the Landsat Thematic Mapper the visible blue band (0.45 to 0.52 μm) can be affected appreciably by comparison to the middle infrared band (1.55 to 1.75 μm).
 - This leads to a loss in calibration of the set of brightnesses associated with a particular pixel.

Instrumentation Errors

- Radiometric errors within a band and between bands can also be caused by the design and operation of the **sensor system**.
 - Band to band errors from this source are normally ignored by comparison to band to band errors from atmospheric effects. However, **detector system errors** within a band can be quite severe and often **require correction** to render an image product useful.
 - An ideal radiation detector *should have a linear transfer characteristic*. However real detectors will have some degree of nonlinearity (ignored here) and will also give a small signal out (dark current offset), see Figure (a), even when no radiation is being detected.
 - Whiskbroom (raster scan) remote sensors involve a *multitude of detectors*. In the case of the Landsat MSS there were 6 per band, for the Landsat TM there are 16 per band.
 - Pushbroom detectors (linear cameras) can have hundreds to thousands of receptors in the swath direction.
 - Each of these detectors will have slightly different transfer characteristics, as described by their gains and offsets, as shown in Figure (b). This could cause *image striping* artifacts either in the along swath direction (whiskbroom scanning) or in the across swath direction (for pushbroom scanning).

Whiskbroom vs Pushbroom
<https://svs.gsfc.nasa.gov/12754>



Striping (or banding) artifacts (along swath direction)



FIGURE Horizontal banding effects can be seen on this Landsat-4 TM band 1 image of part of the High Peak area of Derbyshire, UK. The banding is due to detector imbalance. As there are 16 detectors per band, the horizontal banding pattern repeats every 16th scan line. The image has been contrast-stretched (Section 5.3) in order to emphasise the banding effect. See Section 4.2.2 for more details. Original data courtesy of NASA and USGS.

Striping (or banding) artifacts (across swath direction)

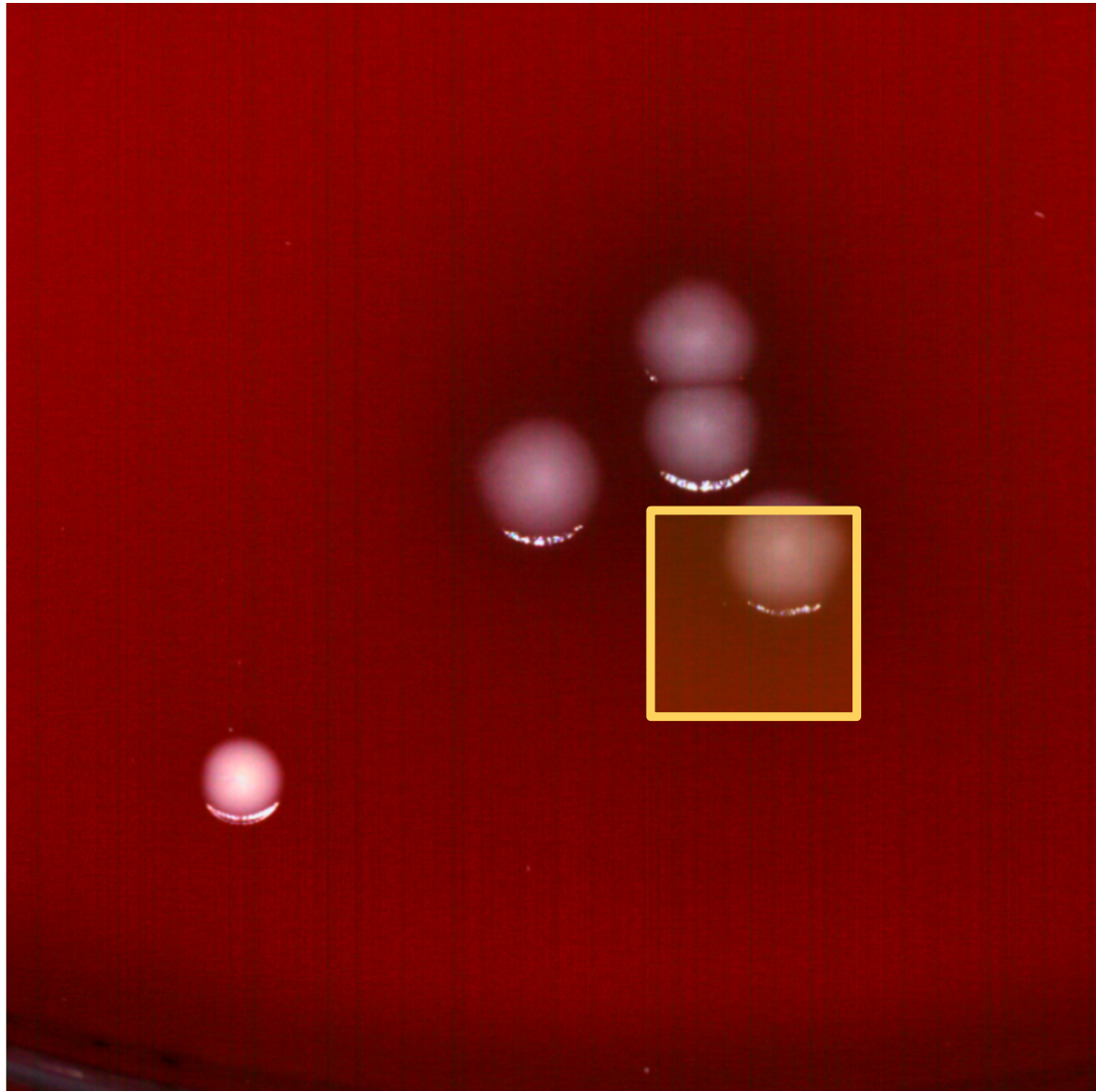


FIGURE Striping artifacts generated by pushbroom acquisition (RGB linear camera) of a bacterial culturing plate (WASPLab – Copan, Italy)

CORRECTION OF RADIOMETRIC DISTORTION

In contrast to geometric correction, in which all sources of error are often rectified together, radiometric correction procedures must be *specific to the nature of the distortion*.

Correction of Atmospheric Effects

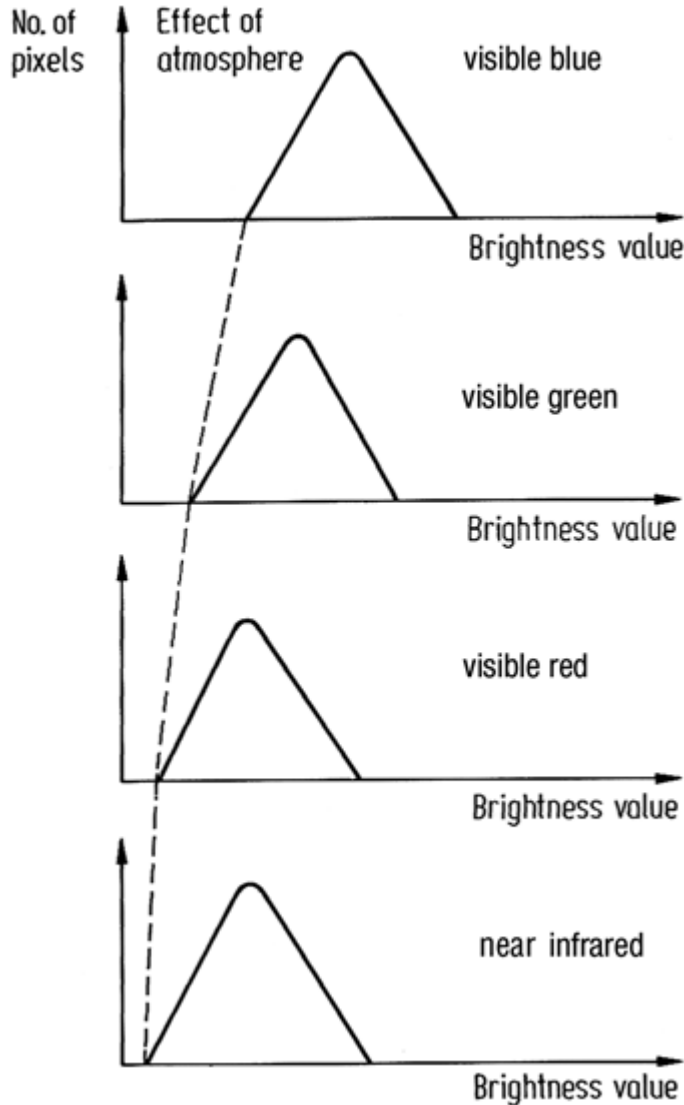
□ **Detailed Correction** of Atmospheric Effects

- See example on the textbook. The example is based on the precise knowledge of some ancillary information such as temperature, relative humidity, atmospheric pressure, visibility and solar zenith angle... and on the exploitation of an atmosphere effects model.

□ **Bulk Correction** of Atmospheric Effects

- In many cases detailed correction for the scattering and absorbing effects of the atmosphere is not required, and often the necessary ancillary information such as visibility and relative humidity is not readily available. In this case an approximate correction is typically carried out.
- If the effect of the atmosphere is judged to be a problem in imagery, approximate bulk correction can be carried out in the following manner.
 - First it is assumed that each band of data for a given scene should have contained some pixels at or close to zero brightness value but that atmospheric effects, and especially ***path radiance, has added a constant value to each pixel in a band.***
 - Consequently if histograms are taken of each band the *lowest significant occupied brightness value will be non-zero.*
 - Moreover because path radiance varies as $\lambda^{-\alpha}$ (with α between 0 and 4 depending upon the extent of Mie scattering) *the lowest occupied brightness value will be further from the origin for the lower wavelengths* as depicted in the following Figure.

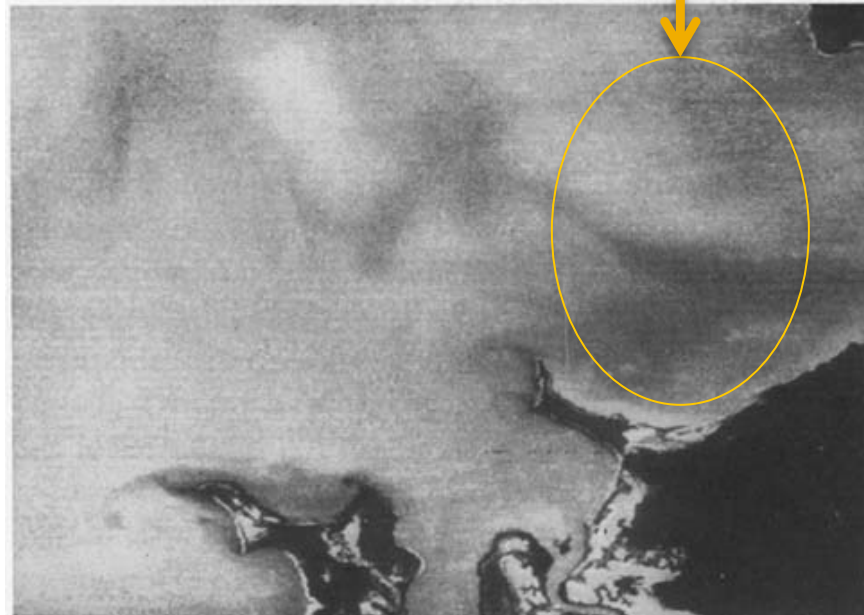
Correction of Atmospheric Effects



- **Correction** consists in
 - first to identifying the amount by which each histogram is “shifted” in brightness away from the origin
 - and then subtracting that amount from each pixel brightness in that band.
- It is clear that *the effect of atmospheric scattering as implied in the histograms of Figure is to lift the overall brightness value of an image in each band.*
 - In the case of a color composite product this will appear as a whitish-bluish haze.
 - Upon correction in the manner just described this haze will be removed and the dynamic range of image intensity will be improved.
 - Consequently, the procedure of atmospheric correction outlined in this section is frequently referred to as ***haze removal***.

Correction of Instrumentation Errors

- Errors in relative brightness such as the within-band line striping referred above and shown in Figure can be rectified to a great extent.
- First it is assumed that the detectors used for data acquisition within a band produce signals **statistically similar to each other**.
- In other words if the *means and standard deviations* are computed for the signals recorded by the detectors then they should be the same (reasonable for whiskbroom detector arrays).
 - This requires the assumption that detail within a band doesn't change significantly over a distance equivalent to that of one scan covered by the set of the detectors (e.g. 474 m for the six scan lines of Landsats 1,2,3 MSS).
 - This is a reasonable assumption so that **differences in those statistics among the detectors can be attributed to gain and offset mismatches**, as discussed above (instrumentation errors slide).
 - These mismatches can be detected by calculating pixel brightness statistics using image data lines, which are known to come from a single detector.



Correction of Instrumentation Errors

- In the case of Landsat MSS this will require the data on every sixth line to be used. In a like manner five other measurements of mean brightness and standard deviation are computed as indications of the performances of the other five MSS detectors.
 - Correction of radiometric mismatches among the detectors can then be effected by adopting one sensor as a reference standard and adjusting the brightness of all pixels recorded by each other detector so that their mean brightnesses and standard deviations match those of the standard detector. This can be done according to

$$y = \frac{\sigma_d}{\sigma_i}x + m_d - \frac{\sigma_d}{\sigma_i}m_i$$

- where x is the old brightness of a pixel and y is its new (destriped) value; m_d and σ_d are the reference values of mean brightness and standard deviation and m_i and σ_i are the mean and standard deviation of the detector under consideration.
- Alternatively, an independent reference mean brightness and standard deviation can be used.
- This can allow a degree of contrast enhancement to be produced during radiometric correction. The method described is frequently referred to as **destriping** (the above Figure gives an example of destriping a Landsat MSS image in this manner).
- The destriping effected by the seen formula is straightforward, but capable only of matching detector responses on the basis of means and standard deviations.
- A more complete destriping procedure should result if the **histograms** of the remaining detectors are matched fully to that of the reference detector (as we will see at a later time). This approach has been used by Weinreb et al. (1989) for destriping weather satellite imagery.

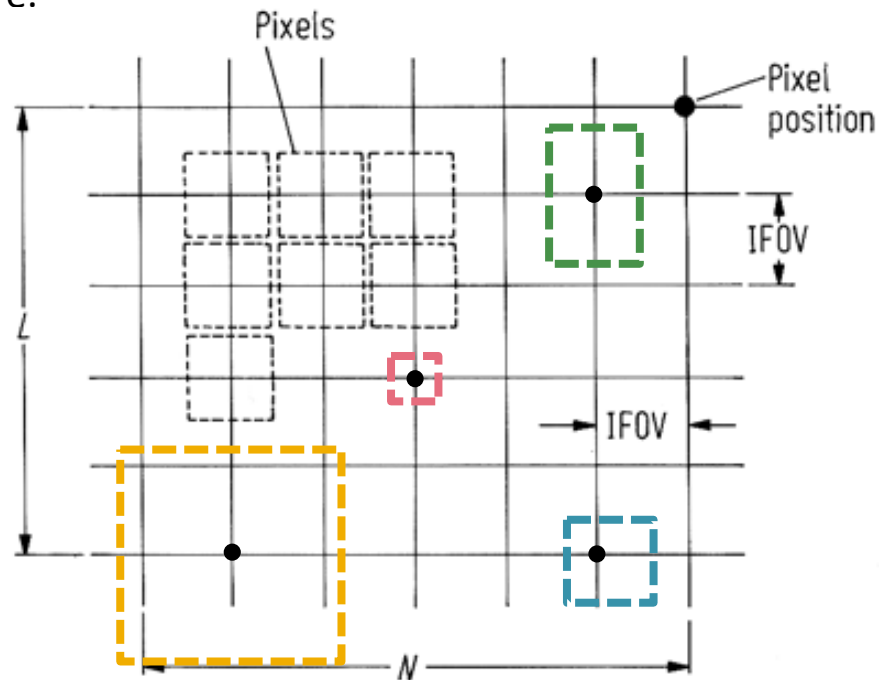
SOURCES OF GEOMETRIC DISTORTION IN REMOTE SENSING DATA

Sources of Geometric Distortion

- There are potentially many more sources of geometric distortion of image data than radiometric distortion and their effects are more severe.
- They can be related to a number of factors, including
 1. *the rotation of the earth during image acquisition,*
 2. *the finite scan rate of some sensors,*
 3. *the wide field of view of some sensors,*
 4. *the curvature of the earth,*
 5. *sensor non-idealities,*
 6. *variations in platform altitude, attitude and velocity, and*
 7. *panoramic effects related to the imaging geometry.*
- It is the purpose here to discuss the nature of the distortions that arise from these effects; later we will discuss means by which the distortions can be compensated.

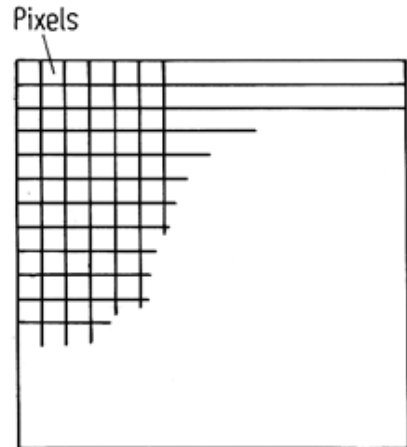
Basic image formation geometry

- To appreciate why geometric distortion occurs, in some cases it is necessary to envisage how an image is formed from sequential lines of image data.
 - If one imagines that a particular sensor records L lines of N pixels each then it would be natural to form the image by laying the L lines down successively one under the other.
 - The grid intersections are the pixel positions and, ideally, the spacing between those grid points is equal to the sensor's instantaneous field of view (IFOV).
 - If the IFOV of the sensor has an aspect ratio of unity – i.e. the pixels are the same size along and across the scan – then this is the same as arranging the pixels for display on a square grid, such as that shown in Figure.
 - However **unity aspect ratio** and pixel size equal to the grid spacing is not automatically granted in linear acquisitions (either raster scan or pushbroom).
 - The system should be **designed** to provide it, or to correct from possible distortion generated by wrong size or bad anisotropic aspect ratio of acquired pixels.
 - In figure different kind of possible distortions are exemplified.

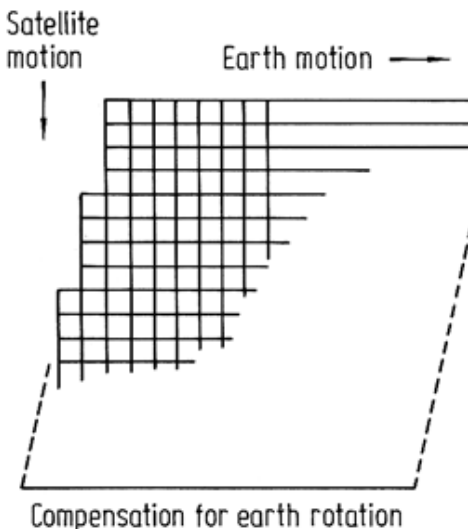


Earth Rotation Effects

- Line scan sensors (such as the Landsat TM) *take a finite time* to acquire a **frame** of image data. The same is true of push broom scanners (such as the SPOT HRV).
- During the frame acquisition time **the earth rotates from west to east**
 - therefore if the lines of image data recorded were arranged for display in the manner of Figure (a), *the later lines would be erroneously displaced to the east*;
 - instead, to give the pixels their correct positions relative to the ground **it is necessary to offset the bottom of the image to the west by the amount of movement of the ground during acquisition**, with all intervening lines displaced proportionately as shown in Fig.(b).
 - this amount depends upon the **relative velocities of the satellite and earth** and the **length of the image frame recorded**.



a



b

Earth Rotation Effects

- An example is presented here for Landsat 7

The angular velocity of the satellite is $\omega_0 = 1.059 \text{ mrad s}^{-1}$ so that a nominal $L = 185 \text{ km}$ frame on the ground is scanned in

$$t_s = L/(r_e \omega_0) = 27.4 \text{ s}$$

where r_e is the radius of the earth (6.37816 Mm).

The surface velocity of the earth is given by

$$v_e = \omega_e r_e \cos \lambda$$

where λ is latitude and ω_e is the earth rotational velocity of $72.72 \mu\text{rad s}^{-1}$. At Sydney, Australia $\lambda = 33.8^\circ$ so that

$$v_e = 385.4 \text{ ms}^{-1}$$

During the frame acquisition time the surface of the earth moves to the east by

$$\Delta x_e = v_e t_s = 10.55 \text{ km at } 33.8^\circ \text{S latitude}$$

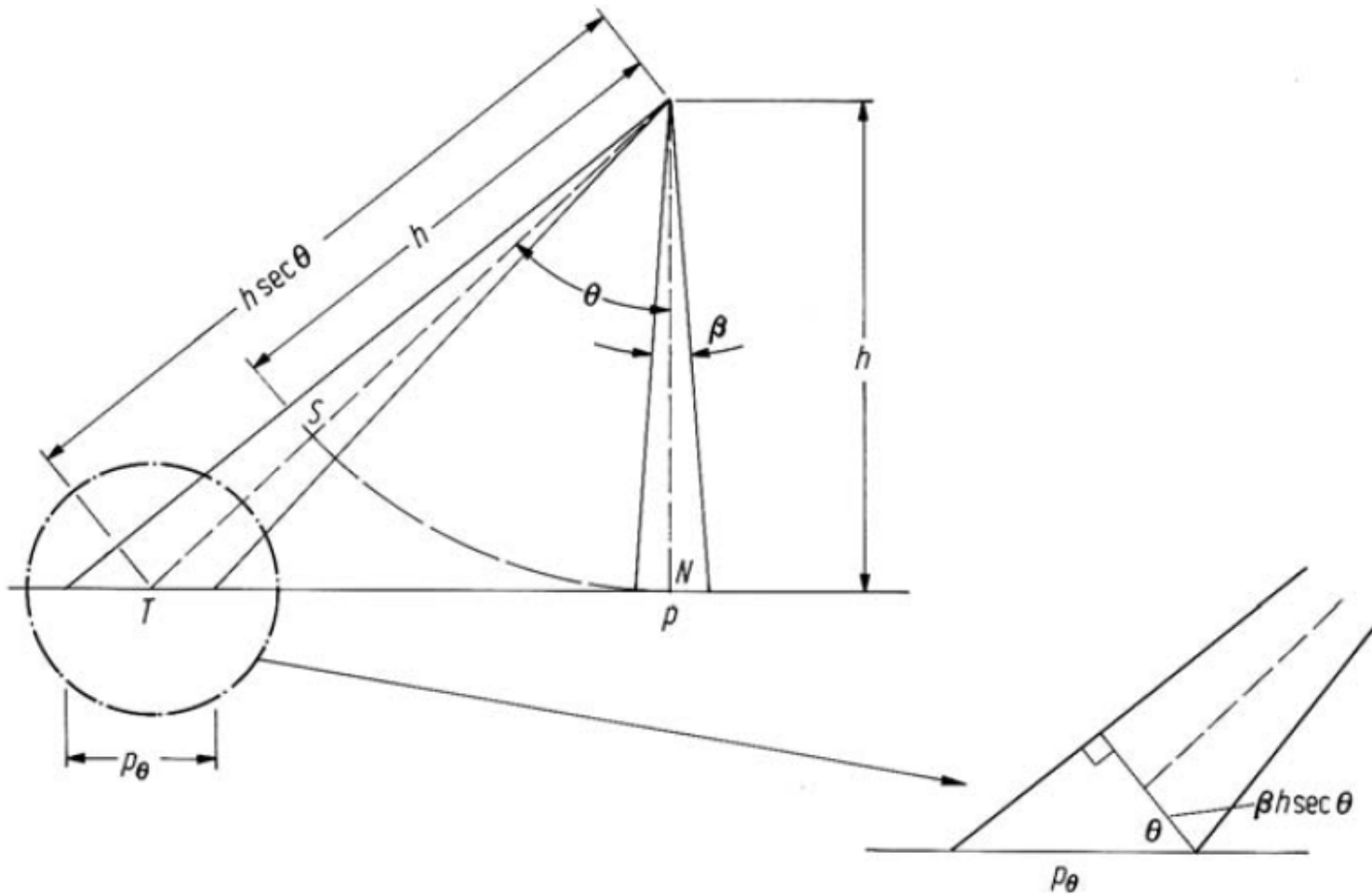
This represents 6% of the frame size. Since the satellite does not pass directly north-south this movement has to be corrected by the inclination angle. At Sydney this is approximately 11° so that the effective sideways movement of the earth is

$$\Delta_x = \Delta x_e \cos 11^\circ = 10.34 \text{ km}$$

Consequently if steps are not taken to correct an image from Landsat 7 for the effect of earth rotation then the image will contain about a 6% skew distortion to the east.

Panoramic Distortion

- For scanners used on spacecraft and aircraft remote sensing platforms the angular IFOV is constant. As a result the effective pixel size on the ground is larger at the extremities of the scan than at nadir, as illustrated in Figure.

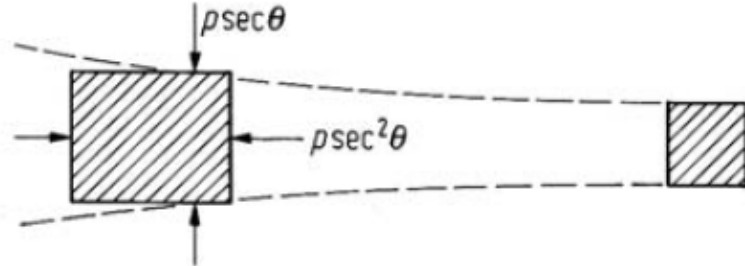


Panoramic Distortion

- In particular, if the IFOV is β and the pixel dimension at nadir is p then its **dimension in the scan direction** at a scan angle of ϑ as shown is

$$p_\vartheta = \beta h \sec^2 \vartheta = p \sec^2 \vartheta,$$

where h is altitude,



while its **dimension across the scan line** is $p \sec \vartheta$.

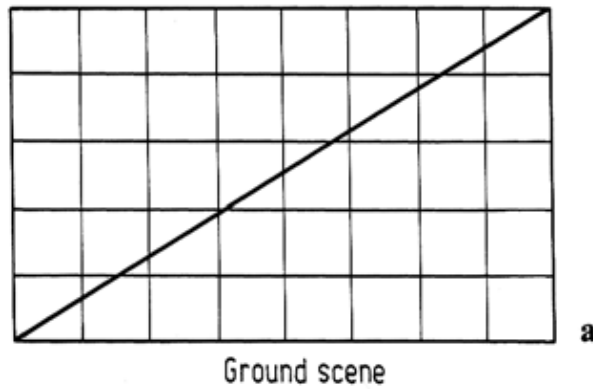
- For small values of ϑ these effects are negligible. For example, for Landsat 7 the largest value of ϑ is approximately 7.5° so that $p_\vartheta = 1.02 p$.
 - However for systems with larger fields of view, such as [MODIS](#) and aircraft scanners, the effect can be quite severe.
 - For an aircraft scanner with $\text{FOV} = 80^\circ$ the distortion in pixel size along the scan line is $p_\vartheta = 1.70 p$ – i.e. the region on the ground measured at the extremities of the scan is 70% larger laterally than the region sensed at nadir.
-
- When the image data is arranged on a regular grid, the displayed pixels are equal across the scan line whereas the equivalent ground areas covered are not.
 - This gives a **geometric compression** of the image data towards its edges.

Panoramic Distortion

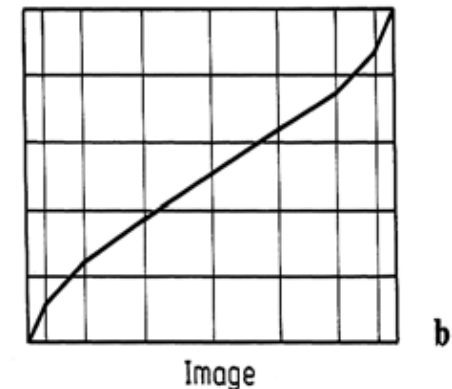
- There is a **second** distortion introduced with wide field of view systems and that relates to **pixel positions across the scan line**.
 - The scanner records pixels at constant angular increments, however the spacings of the effective pixels on the ground increase with scan angle.
 - For example if the pixels are recorded at an angular separation equal to the IFOV of the sensor then at nadir the pixels centres are spaced p apart. At a scan angle ϑ the pixel centres will be spaced $p \sec^2 \vartheta$ apart as can be ascertained from the above Figure.
- Thus by placing the pixels on a uniform display grid the image will suffer an **across track compression**.
 - Again the effect for small angular field of view systems will be negligible in terms of the relative spacing of adjacent pixels.
 - However when the effect is compounded to determine the location of a pixel at the swath edge relative to nadir the error can be significant.
 - This can be determined by computing the length of the **arc $SN = \vartheta h$** in the above Figure, S being the position to which the pixel at T would appear to be moved if the data is arrayed uniformly.
 - It can be shown readily that **$SN/TN = \vartheta / \tan \vartheta$** this being the degree of across track scale distortion.
- In the case of Landsat 7 $(\vartheta / \tan \vartheta)_{\max} = 0.9936$.
 - *This indicates that a pixel at the swath edge (92.5 km from the sub-nadir point) will be 314 m out of position along the scan line compared with the ground if the pixel at nadir is in its correct location.*

Panoramic Distortion

- These panoramic effects lead to an interesting distortion in the geometry of large field of view systems. To see this consider the uniform mesh shown in Figure (a).
 - Suppose this represents a region on the ground being imaged. For simplicity the cells in the grid could be considered to be features on the ground. Because of the **compression in the image data** caused by displaying equal-sized pixels on a uniform grid as discussed in the foregoing, the uniform mesh will appear as shown in Figure (b).
 - Image pixels are recorded with a constant IFOV and at a constant angular sampling rate. Therefore pixels near the swath edges will contain information in common owing to the **overlapping IFOV**.



Ground scene

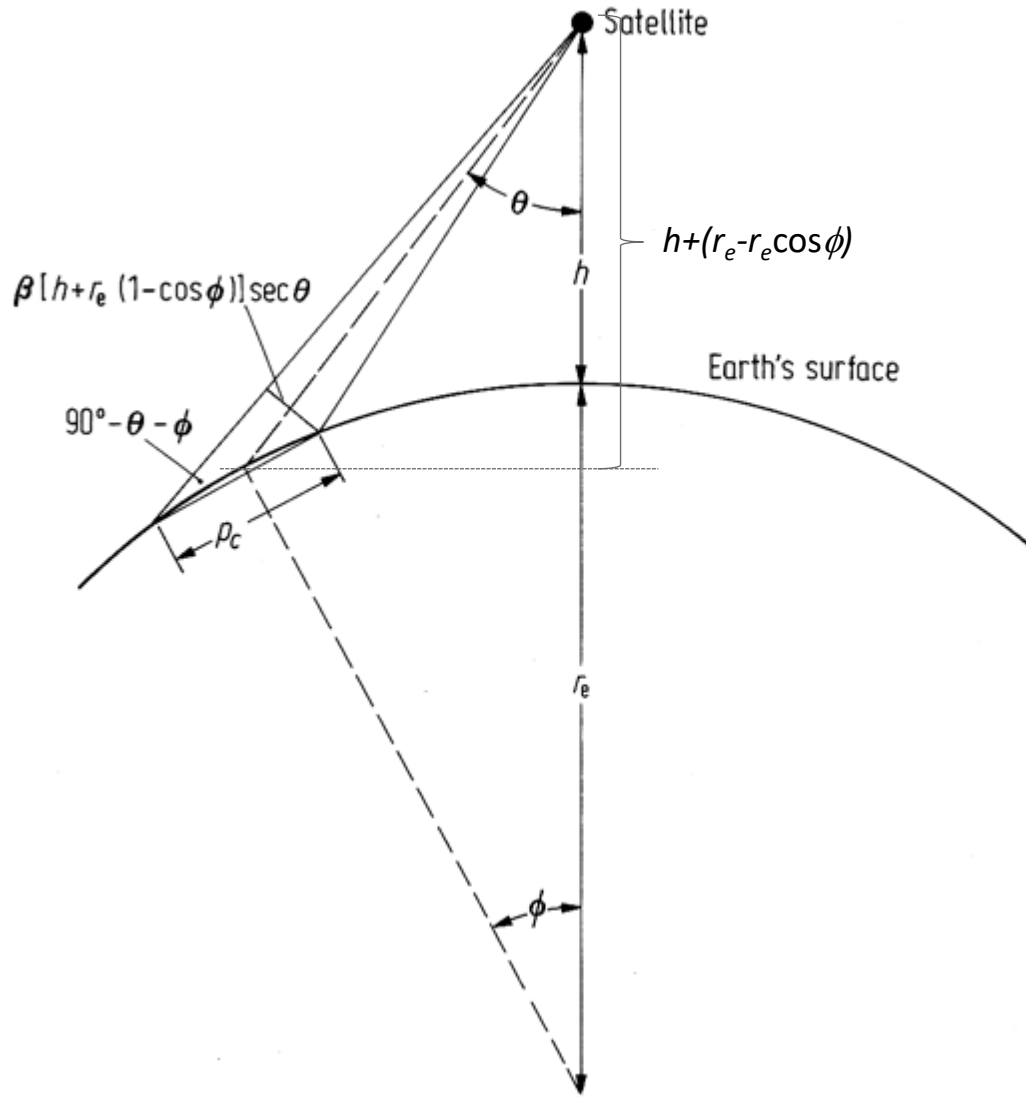


Image

- Linear features such as roads at an angle to the scan direction will appear bent in the displayed image data because of the compression effect. Owing to this, the distortion is also called **S-bend distortion** and can be a common problem with aircraft line scanners.
- Clearly, not only linear features are affected; rather the whole image detail near the swath edges is distorted in this manner.

Earth Curvature

- Aircraft scanning systems, because of their low altitude (and thus the small absolute swath width of their image data), are not affected by earth curvature.
- Neither are space systems on LEO orbits, such as Landsat and SPOT, again because of the *narrowness of their swaths*.
- However, **wide swath width spaceborne imaging systems** are affected.
 - For MODIS with a swath width of 2330 km and an altitude of 705 km it can be shown that the deviation of the earth's surface from a plane amounts to less than 1% over the swath, which seems insignificant. *However it is the inclination of the earth's surface over the swath that causes the greater effect.*



Earth Curvature

- At the edges of the swath the area of the earth's surface viewed at a given angular IFOV is larger than if the curvature of the earth is ignored.
 - The increase in pixel size can be computed by reference to the geometry of the Figure.
 - The pixel dimension in the across the scan line is

$$\beta[h + r_e(1 - \cos \phi)] \sec \theta$$

- The effective pixel size on the inclined earth's surface along the scan direction is

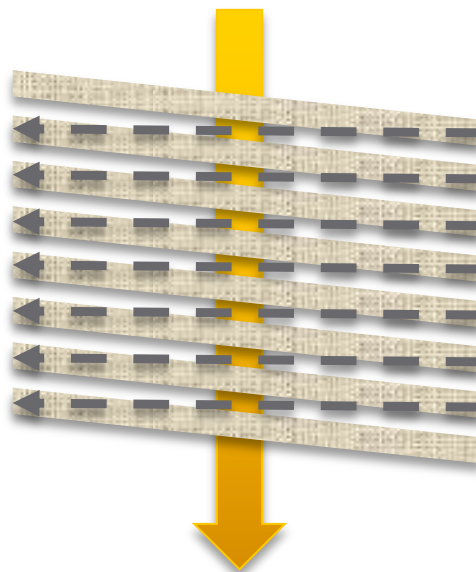
$$p_c = \beta[h + r_e(1 - \cos \phi)] \sec \theta \sec(\theta + \phi)$$

where βh is the pixel size at nadir and ϕ is the angle subtended at the centre of the earth.

- Note that this expression reduces to $p \sec^2 \theta$ (see panoramic distortion) if $\phi = 0$, i.e. if earth curvature is considered negligible.
- Using the NOAA satellite as an example $\vartheta = 54^\circ$ at the edge of the swath and $\phi = 12^\circ$. This shows that the effective pixel size in the along scan direction is 2.89 times larger than that at nadir when earth curvature is ignored, but is 4.94 times that at nadir when the effect of earth curvature is included.
- This demonstrates that **earth curvature introduces a significant additional compressive distortion in the image data acquired by satellites such as [NOAA](#)** when an image is constructed on a uniform grid.
- The effect of earth curvature in the along track direction is negligible.

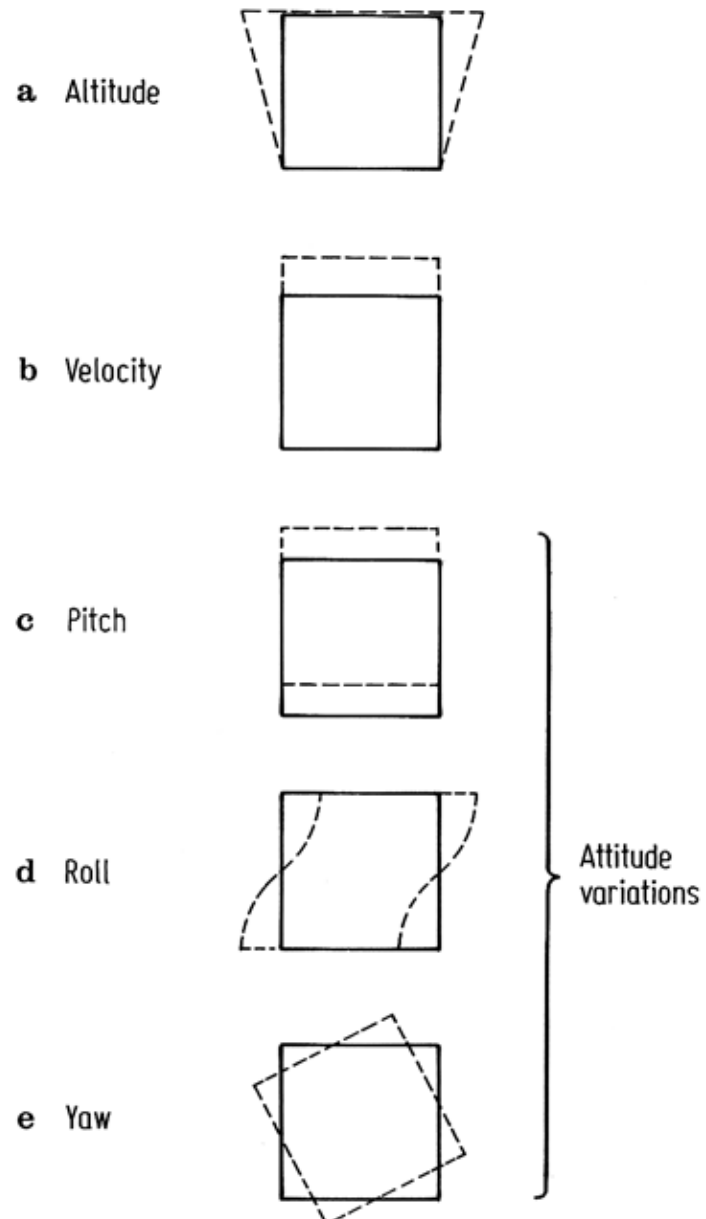
Scan Time Skew

- Mechanical line scanners such as the Landsat MSS and TM require a finite time to scan across the swath.
- During this time the satellite is moving forward leading to a skewing in the along track direction.
 - As an illustration of the magnitude of the effect, the time required to record one MSS scan line of data is 33 ms. During this time the satellite travels forward by 213 m at its equivalent ground velocity of 6.467 km s^{-1} .
 - As a result the end of the scan line is advanced by this amount compared with its start.

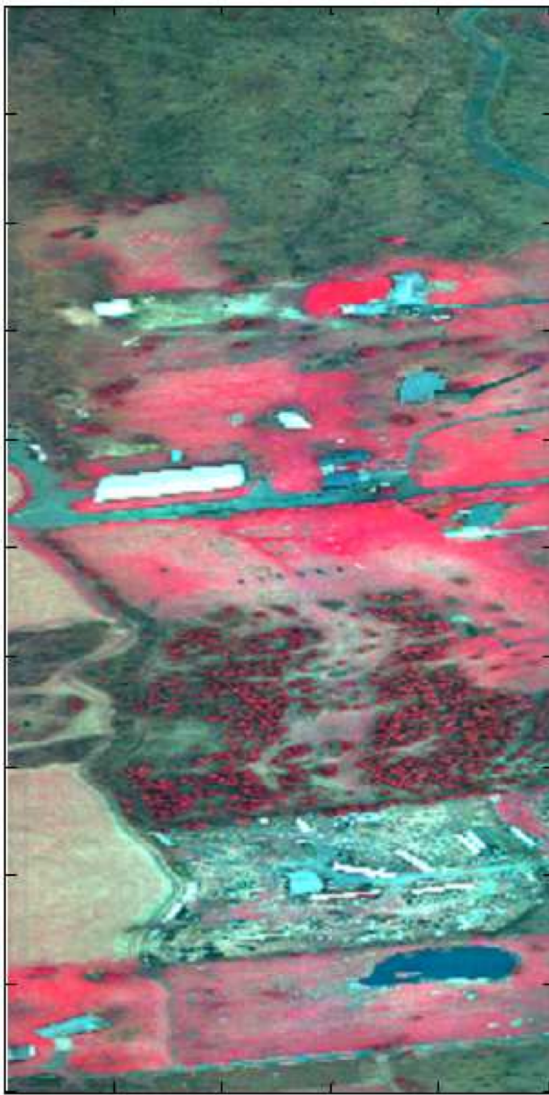


Variations in Platform Altitude, Velocity and Attitude

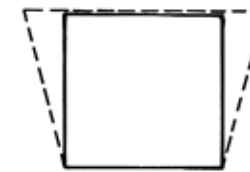
- **Variations in the elevation or altitude** of a remote sensing platform lead to a scale change at constant angular IFOV and field of view; the effect is illustrated in Fig.(a) for an increase in altitude with travel at a rate that is slow compared with a frame acquisition time.
- Similarly, if the platform forward **velocity changes**, a scale change occurs in the along track direction. This is depicted in Fig.(b) again for a change that occurs slowly. For a satellite platform, orbit velocity variations can result from orbit eccentricity and the non-sphericity of the earth.
- Platform **attitude changes** can be resolved into **yaw, pitch and roll** during forward travel. These lead to image rotation, along track and across track displacement as noted in Fig.(c–e).



Variations in Platform Altitude, Velocity and Attitude



a Altitude



b Velocity



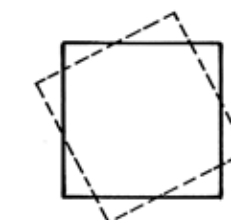
c Pitch



d Roll



e Yaw



Attitude variations

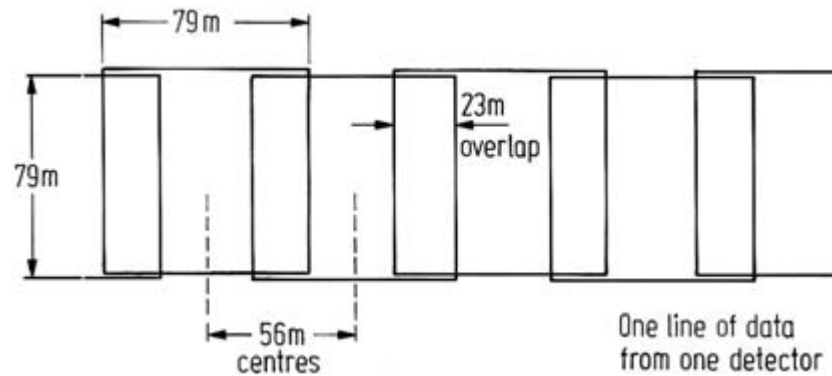
Variations in Platform Altitude, Velocity and Attitude

- While these variations can be described mathematically, at least in principle, a knowledge of the platform **ephemeris** is required to enable their magnitudes to be computed. In the case of satellite platforms, **ephemeris information is often telemetered to ground receiving stations**. This can be used to apply corrections before the data is distributed.
- Attitude variations in aircraft remote sensing systems can potentially be quite significant owing to **the effects of atmospheric turbulence**. These can occur over a short time, leading to *localised distortions* in aircraft scanner images.
 - Frequently aircraft roll is compensated for in the data stream. This is made possible by having a data window that defines the swath width; this is made smaller than the complete scan of data over the sensor field of view. A gyro mounted on the sensor is then used to move the position of the data window along the total scan line as the aircraft rolls.
 - Pitch and yaw are generally not corrected unless the sensor is mounted on a three axis stabilized platform.



Aspect Ratio Distortion

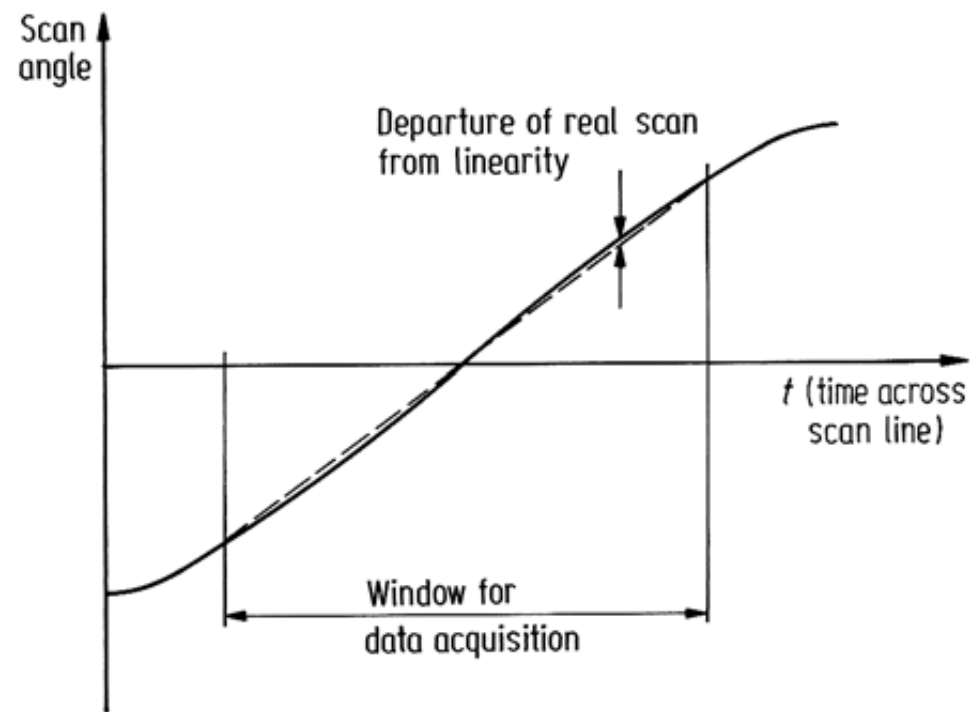
- The aspect ratio of an image (that is, its scale vertically compared with its scale horizontally) can be distorted by mechanisms that lead to overlapping IFOV's.
 - The most notable example of this occurs with the Landsat multispectral scanner, where samples are taken across a scan line too quickly compared with the IFOV. This leads to pixels having 56 metre centres but sampled with an IFOV of 79 m. Consequently the effective pixel size is $79 \text{ m} \times 56 \text{ m}$ and thus is not square (see Figure).
 - As a result, if the pixels recorded by the multispectral scanner are displayed on a regular grid the image will be too wide for its height when related to the corresponding region on the ground. The magnitude of the distortion is $79/56 = 1.411$ so that this is quite a severe error and *must be corrected* for most applications.



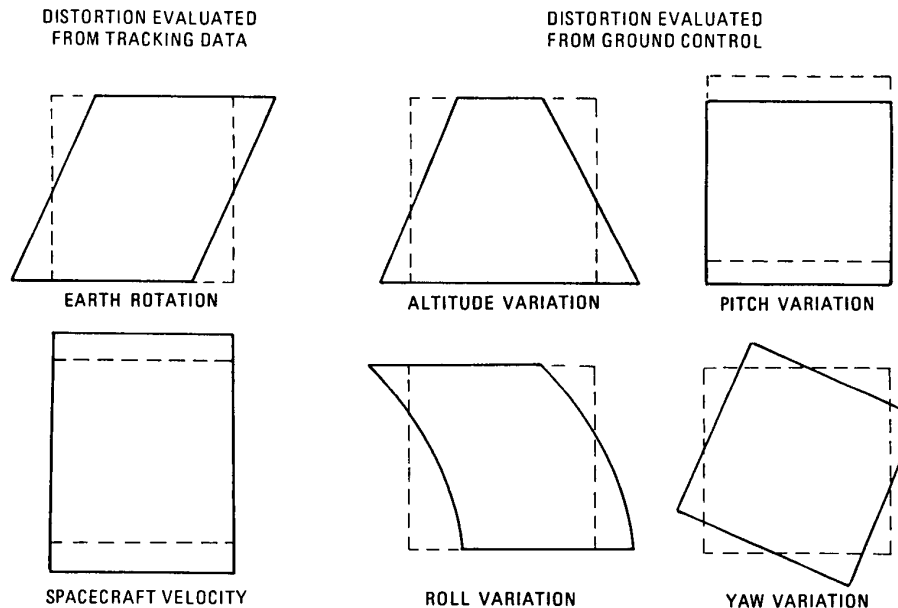
- A similar distortion can occur with aircraft scanners if the velocity of the aircraft is not matched to the scanning rate of the sensor. Either underscanning or overscanning can occur leading to distortion in the alongtrack scale of the image.

Sensor Scan Nonlinearities

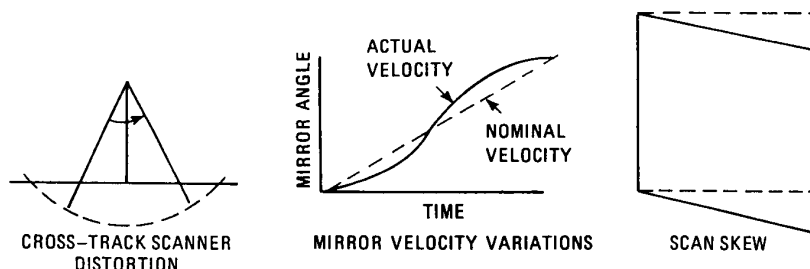
- Line scanners that make use of rotating mirrors, such as the NOAA AVHRR and aircraft scanners, have a *scan rate across the swath that is constant*, to the extent that the scan motor speed is constant.
- Systems that use an **oscillating mirror** however, such as the Landsat thematic mapper, incur some **nonlinearity in scanning near the swath edges** owing to the need for the mirror to slow down and change directions.
 - This effect is depicted in Figure. This can lead to *a maximum displacement in pixel position compared with a perfectly linear scan of about 395 m*, for example, for Landsat multispectral scanner products.
 - Figure shows mirror displacement versus time in an oscillating mirror scanner system. Note that data *acquisition does not continue to the extremes of the scan* so that major nonlinearities are obviated.



Nonsystematic and systematic distortions



A. NONSYSTEMATIC DISTORTIONS. DASHED LINES INDICATE SHAPE OF DISTORTED IMAGE; SOLID LINES INDICATE SHAPE OF RESTORED IMAGE.



B. SYSTEMATIC DISTORTIONS.

FIGURE 7.11 Geometric distortions of Landsat images. From Bernstein and Ferneyhough (1975, Figure 3).

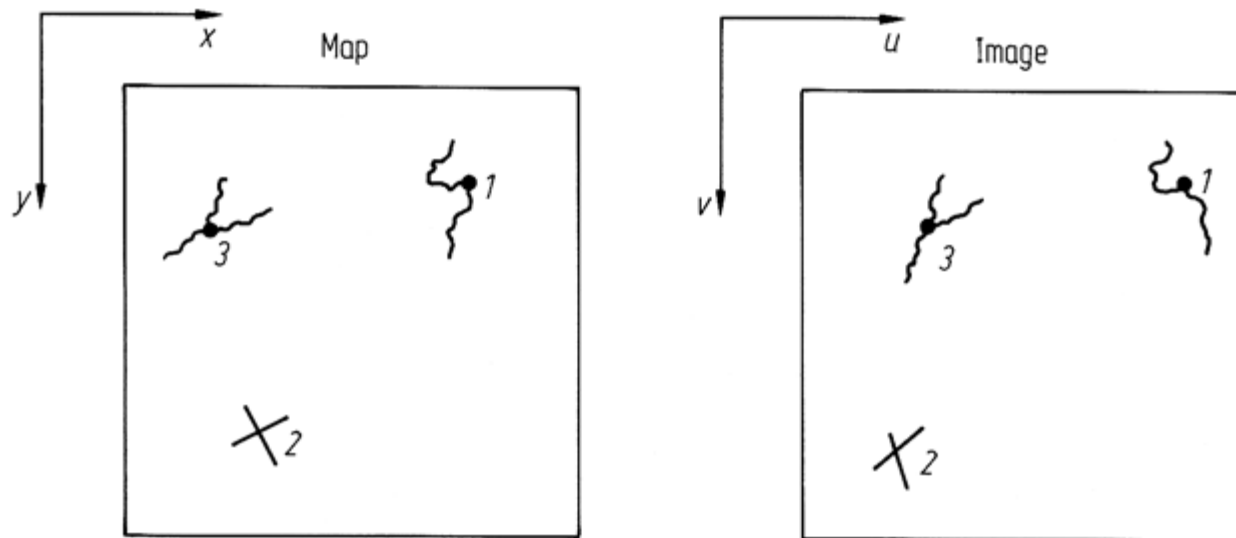
CORRECTION OF GEOMETRIC DISTORTION

Correction of Geometric Distortion – general aspects

- There are two approaches that can be used to correct the various types of geometric distortion present in digital image data.
 1. One is to **model the nature and magnitude of the sources of distortion** and use these models to establish correction formulae. This technique is effective when the types of distortion are well characterized, such as that caused by earth rotation.
 - Correction by mathematical modeling is discussed later.
 2. The second approach depends upon establishing **mathematical relationships between the position of pixels in an image and the corresponding coordinates of those points on the ground** (via a **map**). These relationships can be used to correct the image geometry irrespective of the analyst's knowledge of the source and type of distortion.
 - This procedure will be treated first since it is the most commonly used and, as a technique, is **general and independent of the platform/device** used for data acquisition.
- Before proceeding it should be noted that each band of image data has to be corrected. However, since it can often be assumed that the bands are well registered to each other, steps taken to correct one band in an image, can be used on all remaining bands.

Use of Mapping Polynomials for Image Correction

- An assumption that is made in this procedure is that **there is available a map of the region corresponding to the image, that is correct geometrically.**
 - We then define two Cartesian coordinate systems as shown in Figure. One describes the location of points in the map (x, y) and the other coordinate system defines the location of pixels in the image (u, v).



Use of Mapping Polynomials for Image Correction

- Now suppose that the two coordinate systems can be related via a pair of mapping functions f and g so that

$$u = f(x, y)$$

$$v = g(x, y)$$

- If these functions are known then we could locate a point in the image knowing its position on the map. In principle, the reverse is also true. With this ability we could build up a geometrically correct version of the image in the following manner.
 - First we define a **grid over the map** to act as the grid of pixel centres in the corrected image. This grid is parallel to, or indeed could in fact be, the map coordinate grid itself, described by latitudes and longitudes, UTM coordinates and so on. For simplicity we will refer to this grid as the display grid; by definition this is geometrically correct.
 - We then move over the display grid pixel centre by pixel centre and use the mapping functions above **to find the corresponding pixel in the image** for each display grid position. Those pixels are then placed on the display grid. At the conclusion of the process we have a geometrically correct image built up on the display grid utilizing the original image as a source of pixels.
- While the process is a straightforward one there are some practical **difficulties that must be addressed**.
 - First we do not know the explicit form of the mapping functions of f and g .
 - Secondly, even if we did, they may not point exactly to a pixel in the image corresponding to a display grid location; instead some form of *interpolation* may be required.

Use of Mapping Polynomials for Image Correction

Mapping Polynomials and Ground Control Points

- Since explicit forms for the mapping functions f and g in are *not known* they are generally chosen as simple polynomials of first, second or third degree.

- For example, in the case of second degree

$$u = a_0 + a_1x + a_2y + a_3xy + a_4x^2 + a_5y^2$$

$$v = b_0 + b_1x + b_2y + b_3xy + b_4x^2 + b_5y^2$$

- Sometimes orders higher than three are used but care must be taken to avoid the introduction of worse errors than those to be corrected, as will be noted later.
 - If the coefficients a_i and b_i were known then the mapping polynomials could be used to relate any point in the map to its corresponding point in the image as in the foregoing discussion.
 - At present however these coefficients are unknown.

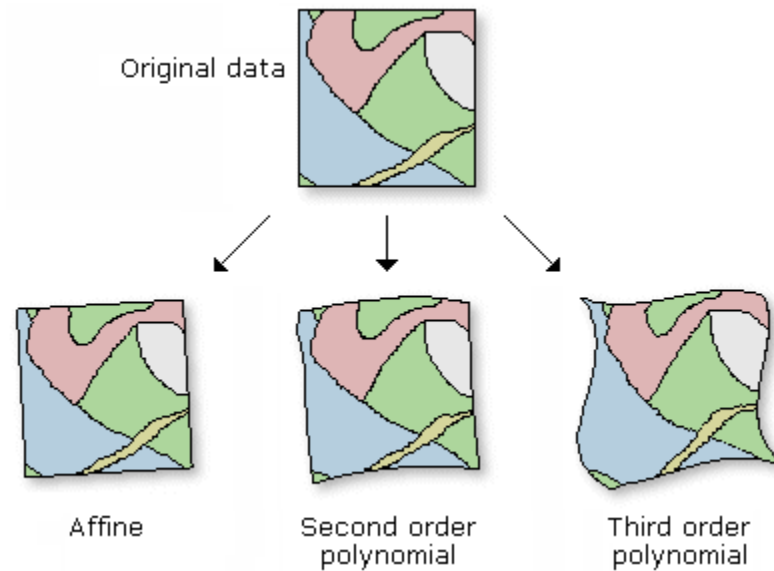
- Values can be **estimated** by identifying sets of features on the map that can also be identified on the image.

- These features, often referred to as **ground control points** (*GCP's*), are well-defined and spatially small and could be
 - road intersections,
 - airport runway intersections,
 - bends in rivers,
 - prominent coastline features and the like...

Use of Mapping Polynomials for Image Correction

Mapping Polynomials and Ground Control Points

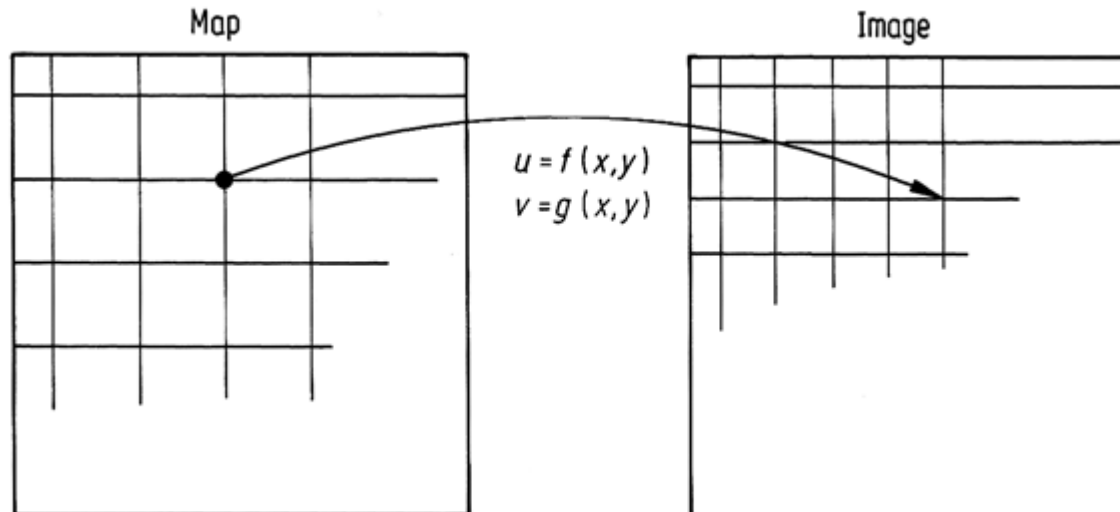
- Enough of these control points are chosen (as pairs – on the map and image as depicted in the above Figure) so that the polynomial coefficients can be estimated by substitution into the mapping polynomials to yield sets of equations in those unknowns.
 - The above equations show that the *minimum number* required for second order polynomial mapping is six.
 - Likewise a minimum of three is required for first order (affine) mapping and ten for third order mapping.
 - In practice however significantly more than these are chosen and the coefficients are evaluated using **least squares estimation**. In this manner any control points that contain significant positional errors either on the map or in the image will not have an undue influence on the polynomial coefficients.



Use of Mapping Polynomials for Image Correction

Resampling

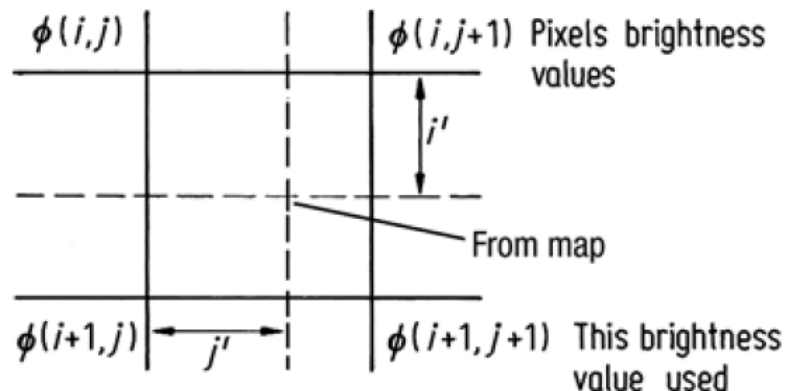
- Having determined the mapping polynomials explicitly by use of the ground control points, the next step is to find points in the image corresponding to each location in the pixel grid previously defined over the map.
 - The spacing of that grid is chosen according to the pixel size required in the corrected image and need not be the same as that in the original geometrically distorted version.
 - For the moment suppose that the points located in the image correspond exactly to image pixel centres. Then those pixels are simply transferred to the appropriate locations on the display grid to build up the rectified image. This is the case in Figure.



Use of Mapping Polynomials for Image Correction

Interpolation

- As is to be expected, grid centres from the map-registered pixel grid will not usually project to exact pixel centre locations in the image, as shown in the above Figure, and some decision has to be made therefore about what pixel brightness value should be chosen for placement on the new grid.
- Three techniques can be used for this purpose.
 1. ***Nearest neighbor resampling*** simply chooses the actual pixel that has its centre nearest the point located in the image, as depicted in Figure. This pixel is then transferred to the corresponding display grid location. This is the preferred technique if the new image is to be classified since it then consists of the original pixel brightnesses, simply rearranged in position to give a correct image geometry.



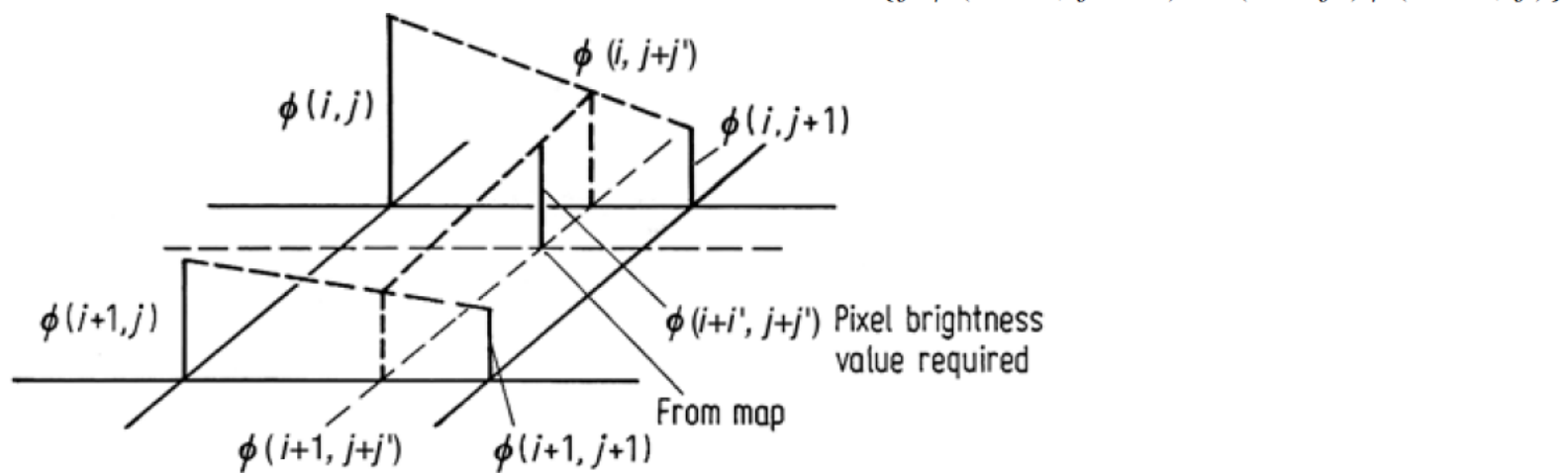
Use of Mapping Polynomials for Image Correction

Interpolation

2. **Bilinear interpolation** uses three linear interpolations over the four pixels that surround the point found in the image corresponding to a given display grid position.

- The process is illustrated in Figure: Two linear interpolations are performed along the scan lines to find the interpolants $\phi(i, j + j')$ and $\phi(i + 1, j + j')$ as shown.
- These are given by $\phi(i, j + j') = j'\phi(i, j + 1) + (1 - j')\phi(i, j)$
 $\phi(i + 1, j + j') = j'\phi(i + 1, j + 1) + (1 - j')\phi(i + 1, j)$

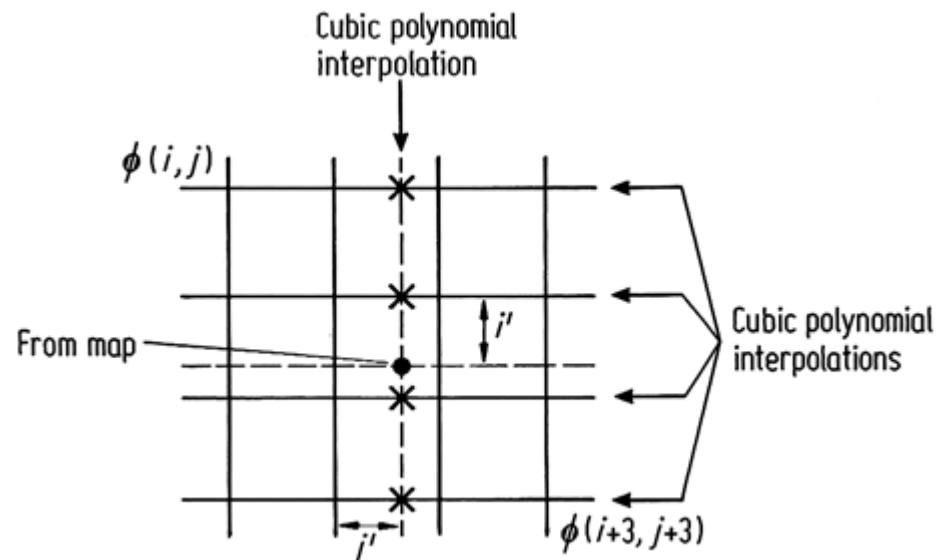
where ϕ is pixel brightness and $(i+i', j+j')$ is the position at which an interpolated value for brightness is required. The position is measured with respect to (i, j) and assumes a grid spacing of unity in both directions. The final step is to interpolate linearly over $\phi(i, j + j')$ and $\phi(i + 1, j + j')$ to give $\phi(i + i', j + j') = (1 - i')\{\phi(i, j + 1) + (1 - j')\phi(i, j)\} + i'\{\phi(i + 1, j + 1) + (1 - j')\phi(i + 1, j)\}$



Use of Mapping Polynomials for Image Correction

Interpolation

- **Cubic convolution interpolation** uses the surrounding sixteen pixels.
 - Cubic polynomials are fitted along the four lines of four pixels surrounding the point in the image, as depicted in Figure to form four interpolants.
 - A fifth cubic polynomial is then fitted through these to synthesize a brightness value for the corresponding location in the display grid.
 - The actual form of polynomial that is used for the interpolation is derived from considerations in sampling theory and issues concerned with constructing a continuous function (i.e. interpolating) from a set of samples.
 - An excellent treatment of the problem has been given by Shlien (1979), who discusses several possible cubic polynomials that could be used for the interpolation process and who also demonstrates that the interpolation is a convolution operation.
 - Based on the choice of a suitable polynomial (attributable to Simon (1975)) the algorithm that is used to perform cubic convolution interpolation is (Moik, 1980): →



Use of Mapping Polynomials for Image Correction

Interpolation

$$\begin{aligned} \rightarrow \quad \phi(i, j + 1 + j') = & j' \{ j' [j' [\phi(i, j + 3) - \phi(i, j + 2) + \phi(i, j + 1) - \phi(i, j)] \\ & + [\phi(i, j + 2) - \phi(i, j + 3) - 2\phi(i, j + 1) + 2\phi(i, j)]] \\ & + [\phi(i, j + 2) - \phi(i, j)] \} \\ & + \phi(i, j + 1) \end{aligned}$$

- This expression is evaluated for each of the four lines of four pixels depicted in Figure, to yield the four interpolants $\phi(i, j + 1 + j')$, $\phi(i + 1, j + 1 + j')$, $\phi(i + 2, j + 1 + j')$, $\phi(i + 3, j + 1 + j')$.
- These are then interpolated vertically according to

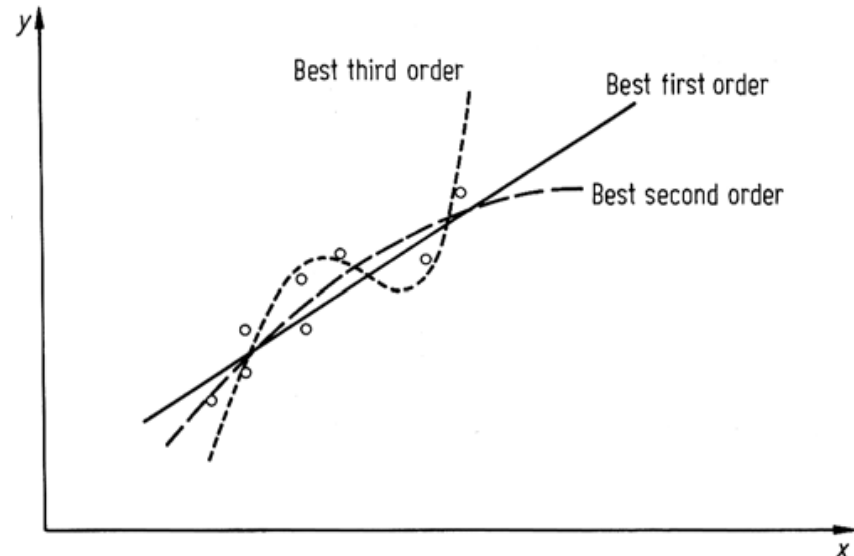
$$\begin{aligned} \phi(i + 1 + i', j + 1 + j') = & i' \{ i' [i' [\phi(i + 3, j + 1 + j') - \phi(i + 2, j + 1 + j')] \\ & + \phi(i + 1, j + 1 + j') - \phi(i, j + 1 + j')] \\ & + [\phi(i + 2, j + 1 + j') - \phi(i + 3, j + 1 + j')] \\ & - 2\phi(i + 1, j + 1 + j') + 2\phi(i, j + 1 + j')] \\ & + [\phi(i + 2, j + 1 + j') - \phi(i, j + 1 + j')] \} \\ & + \phi(i + 1, j + 1 + j') \end{aligned}$$

- **Cubic convolution interpolation, or resampling, yields an image product that is generally smooth in appearance and is often used if the final product is to be treated by photo-interpretation.**
- **However since it gives pixels on the display grid, with brightnesses that are interpolated from the original data, it is not recommended if classification is to follow since the new brightness values may be too different from the actual radiance values detected by the satellite sensors.**

Use of Mapping Polynomials for Image Correction

Choice of Control Points

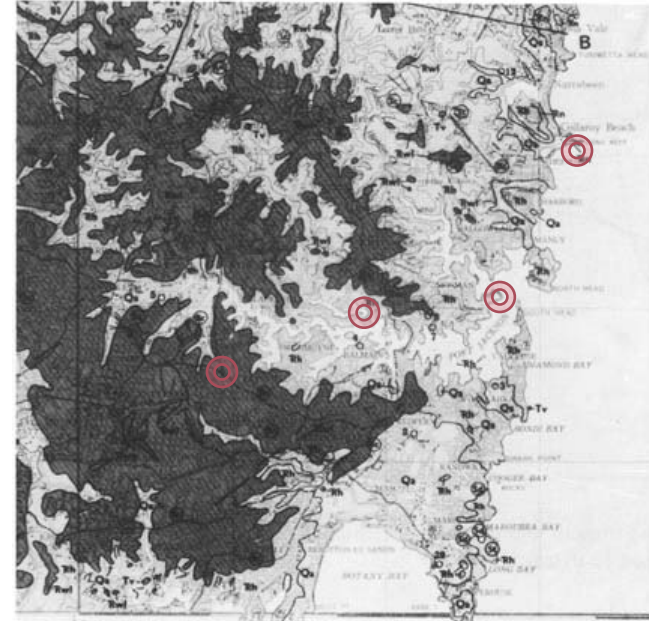
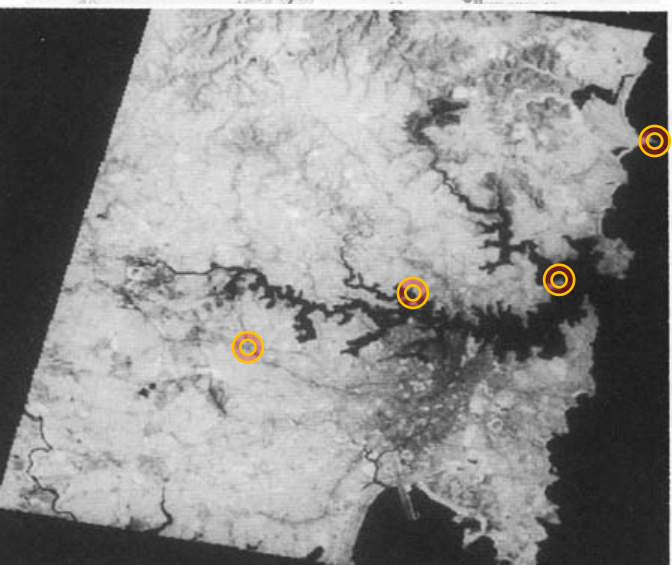
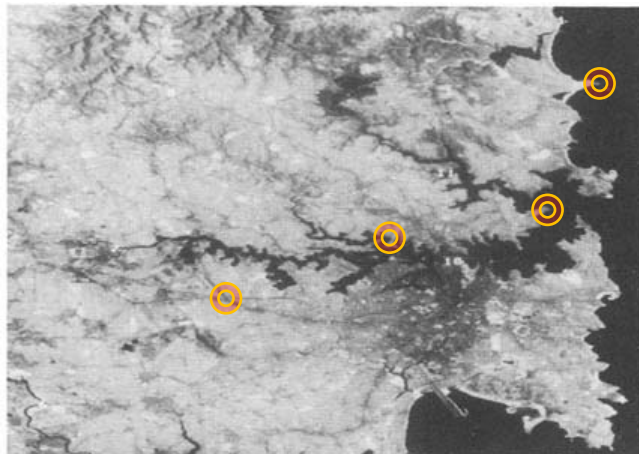
- Enough well defined control point pairs must be chosen in rectifying an image to ensure that accurate mapping polynomials are generated.
- However **care must also be given to the locations of the points.**
 - A general rule is that **there should be a distribution of control points around the edges of the image** to be corrected with a scattering of points over the body of the image.
 - This is necessary to ensure that the mapping polynomials are well-behaved over the image.
- This concept can be illustrated by considering an example from curve fitting.
 - While the nature of the problem is different the undesirable effects that can be generated are similar. In Figure is illustrated a set of data points in a graph through which first order (linear), second order and third order curves are depicted.
 - Note that as the order is higher the curves pass closer to the points.
 - In contrast the cubic curve can deviate markedly from the trend when used as an extrapolator, and the linear fit seem to be the most acceptable one in this case.



Use of Mapping Polynomials for Image Correction

Example: Map - Landsat MSS registration

- A Map and a Landsat MSS image segment to be registered. The result is obtained from **second order mapping polynomials** and a set of **11 control points**.
 - Estimated error 56m easting, 63m northing which are smaller than the pixel size.
 - See Richards' book for more details
 - Residual high errors on single control points should be evaluated individually
 - Poor placement
 - Local distortions, etc.



Mathematical Modelling

- If a particular distortion in image geometry can be represented mathematically then the mapping functions $u = f(x, y)$ and $v = g(x, y)$ can be specified explicitly.
- This obviates the need to choose arbitrary polynomials and to use control points to determine the polynomial coefficients (as seen before) .
- In the following some of the more common distortions are treated from this point of view.
- However, rather than commence with expressions that relate image coordinates (u, v) to map coordinates (x, y) it is probably simpler conceptually to start the otherway around, i.e. to model what the true (map) positions of pixels should be, given their positions in an image.
- This expression can then be inverted if required to allow the image to be resampled on to the map grid.

Mathematical Modelling

Aspect Ratio Correction

- The easiest source of distortion to model is that caused by the 56 m equivalent ground spacing of the 79 m × 79 m equivalent pixels in the Landsat MS scanner.
 - As noted this leads to an image that is too wide for its height by a factor of $79/56 = 1.411$.
 - Consequently to produce a geometrically correct image either the vertical dimension has to be expanded by this amount or the horizontal dimension must be compressed.
 - We will consider the former. This requires that the pixel axis horizontally be left unchanged but that the axis vertically be scaled. This can be expressed conveniently in matrix notation as

$$\begin{bmatrix} x \\ y \end{bmatrix} = \begin{bmatrix} 1 & 0 \\ 0 & 1.411 \end{bmatrix} \begin{bmatrix} u \\ v \end{bmatrix}$$

- and this can be inverted in

$$\begin{bmatrix} u \\ v \end{bmatrix} = \begin{bmatrix} 1 & 0 \\ 0 & 0.709 \end{bmatrix} \begin{bmatrix} x \\ y \end{bmatrix}$$

- Thus, as with the techniques based on control points, a display grid is defined over the map (with coordinates (x, y)) and the above transform is used to find the corresponding location in the image (u, v) . The already seen interpolation techniques are then used to generate brightness values for the display grid pixels.

Mathematical Modelling

Earth Rotation Skew Correction

- To correct for the effect of earth rotation it is necessary to implement a shift of pixels to the left that is dependent upon the particular line of pixels, measured with respect to the top of the image.
 - Their line addresses as such (v) are not affected.
 - From what we have already seen, these corrections are implemented by

$$\begin{bmatrix} x \\ y \end{bmatrix} = \begin{bmatrix} 1 & \alpha \\ 0 & 1 \end{bmatrix} \begin{bmatrix} u \\ v \end{bmatrix}$$

with $\alpha = -0.056$ for Sydney, Australia.

- This can be implemented in an approximate sense by making one-pixel shift to the left every 17 lines of image data measured down from the top, or alternatively, and more precisely, the expression can be inverted to give

$$\begin{bmatrix} u \\ v \end{bmatrix} = \begin{bmatrix} 1 & -\alpha \\ 0 & 1 \end{bmatrix} \begin{bmatrix} x \\ y \end{bmatrix} = \begin{bmatrix} 1 & 0.056 \\ 0 & 1 \end{bmatrix} \begin{bmatrix} x \\ y \end{bmatrix}$$

which again is used with an interpolation procedures to generate display grid pixels.

Mathematical Modelling

Image Orientation to North-South

- Although not strictly a geometric distortion it is an inconvenience to have an image that is corrected for most major effects but is not oriented vertically in a north-south direction.
 - It will be recalled for example that the Landsat orbits in particular are inclined to the north-south line by about 9° . (This of course is different with different latitudes).
- To rotate an image by an angle ζ in the counter -or anticlockwise direction (as required in the case of Landsat) it is easily shown that

$$\begin{bmatrix} x \\ y \end{bmatrix} = \begin{bmatrix} \cos \zeta & \sin \zeta \\ -\sin \zeta & \cos \zeta \end{bmatrix} \begin{bmatrix} u \\ v \end{bmatrix}$$

so that

$$\begin{bmatrix} u \\ v \end{bmatrix} = \begin{bmatrix} \cos \zeta & -\sin \zeta \\ \sin \zeta & \cos \zeta \end{bmatrix} \begin{bmatrix} x \\ y \end{bmatrix}$$

Mathematical Modelling

Correction of Panoramic Effects

- The discussion about panoramic distortion makes note of the pixel positional error that results from scanning with a fixed IFOV at a constant angular rate. In terms of map and image coordinates, the distortion can be described by

$$\begin{bmatrix} x \\ y \end{bmatrix} = \begin{bmatrix} \tan \vartheta / \theta & 0 \\ 0 & 1 \end{bmatrix} \begin{bmatrix} u \\ v \end{bmatrix}$$

- where ϑ is the instantaneous scan angle, which in turn can be related to x or u , namely $x = h \tan \vartheta$, $u = h\vartheta$, where h is altitude (in this case u means undistorted, i.e. proportional to ϑ).
 - Consequently, resampling can be carried out according to

$$\begin{bmatrix} u \\ v \end{bmatrix} = \begin{bmatrix} \theta \cot \theta & 0 \\ 0 & 1 \end{bmatrix} \begin{bmatrix} x \\ y \end{bmatrix} = \begin{bmatrix} h/x \tan^{-1}(x/h) & 0 \\ 0 & 1 \end{bmatrix} \begin{bmatrix} x \\ y \end{bmatrix}$$

Mathematical Modelling

Combining the Corrections

- Clearly any exercise in image correction usually requires several distortions to be rectified.
 - Using the mapping polynomials techniques for image correction it is assumed that all sources are rectified simultaneously.
 - When employing mathematical modeling, a correction matrix has to be devised for each source considered important, as in the preceding slides, and the set of matrices combined.
 - For example, if the aspect ratio of a Landsat TM image is corrected first, followed by correction of the effect of earth rotation, then the following single linear transformation can be established for resampling

$$\begin{bmatrix} x \\ y \end{bmatrix} = \begin{bmatrix} 1 & \alpha \\ 0 & 1 \end{bmatrix} \begin{bmatrix} 1 & 0 \\ 0 & 1.411 \end{bmatrix} \begin{bmatrix} u \\ v \end{bmatrix}$$
$$= \begin{bmatrix} 1 & 1.411\alpha \\ 0 & 1.411 \end{bmatrix} \begin{bmatrix} u \\ v \end{bmatrix}$$

which for $\alpha = -0.056$ (at Sydney) gives

$$\begin{bmatrix} u \\ v \end{bmatrix} = \begin{bmatrix} 1 & 0.056 \\ 0 & 0.709 \end{bmatrix} \begin{bmatrix} x \\ y \end{bmatrix}$$

IMAGE REGISTRATION

Georeferencing and Geocoding

- Using the correction techniques of the preceding sections an image can be registered to a map coordinate system and therefore have its pixels addressable in terms of **map coordinates** (eastings and northings, or latitudes and longitudes) rather than pixel and line numbers.
- **Other spatial data types**, such as geophysical measurements, image data from other sensors and the like, **can be registered similarly to the map** thus creating a **georeferenced integrated spatial data base** of the type used in a **geographic information system (GIS)**.
- **Nomenclature**
 - ***Image to image registration***: the alignment of an image (slave) to another image (master) of the same area (e.g. taken at different dates and/or with different techniques)
 - ***Rectification or georeferencing***: the alignment of an image to a map (also by geometric distortion correction, in this case we refer to an ***orthorectification***) so that the image is *planimetric*, just like the map.
 - A particular rectification which allow to directly express image pixel addresses in terms of a map coordinate base is often referred to as ***geocoding***.

Image to Image Registration

- Many applications of remote sensing image data require *two or more scenes of the same geographical region, acquired at different dates, to be processed together.*
 - Such a situation arises for example when **changes** are of interest, in which case registered images allow a *pixel-by-pixel comparison* to be made.
- Two images can be registered to each other by registering each to a map coordinate base separately, in the manner demonstrated previously.
- Alternatively, and particularly if georeferencing is not a priority, one image can be chosen as a **master** to which the other, known as the **slave**, is to be registered.
 - Again the already seen techniques are used, however
 - the coordinates (x, y) are now the pixel coordinates in the master image rather than the map coordinates;
 - while, as before, (u, v) are the coordinates of the image to be registered (i.e. the slave).
- An advantage in *image-to-image* registration is that *only one registration step is required* in comparison to two if both are taken back to a map base.

Image to Image Registration

- Manual **GCP selection** and **correspondence search** between two images (or between one image and a map) can be a tedious and time-consuming task
- Today there are several solutions (***feature-point extraction and description techniques***) that allow the latter task or even both to be automatic or semiautomatic (with reasonable reliability and robustness)
- Following, a possible *classification* of automatic or semiautomatic image-to-image registration or GCP localization and correspondence search techniques:
 - Algorithms that uses pixel intensity values directly (rigid or affine registration)
 - Correlation methods
 - Mutual information maximization methods
 - Frequency- or wavelet-domain techniques (rigid or affine registration)
 - **Feature-based methods** that uses *low-level features* such as shapes, edges and corners (both rigid and deformable registration)
 - comprising both manually or semi-automatically selected feature points, like GCPs
 - or automated ones, like SIFT
 - Object-based (*high-level features*) techniques (less used for registration)

Control Point Localisation by Windowed Image Correlation

- To locate the position of a control point in the master image, having identified it in the slave, **(localized) correlation techniques** can be used.
 - The *correlation measure used need not be sophisticated*: a simple similarity check that can be used is to compute the sum of the absolute differences of the slave and master image pixel brightnesses over a local window (around the control point), for each possible location of the window in the search region.
 - In principle a rectangular sample of pixels surrounding the control point in the slave image can be extracted as a window to be correlated with the master image.
 - Because of the spatial properties of the pair of images near the control points a high correlation should occur when the slave window is located over its exact counterpart region in the master, and thus the master location of the control point is identified.
 - Obviously, it is not necessary to move the slave window over the complete master image since the user knows approximately where the control point should occur in the master.
 - Consequently, it is only necessary to specify a search region in the neighborhood of the approximate location.
 - In remote sensing this is also called **sequential similarity detection algorithm** (SSDA) [Bernstein (1983)]
 - Clearly the use of techniques such as these to locate control points depends upon there not being major changes of an uncorrelated nature between the scenes in the vicinity of a control point being tested.

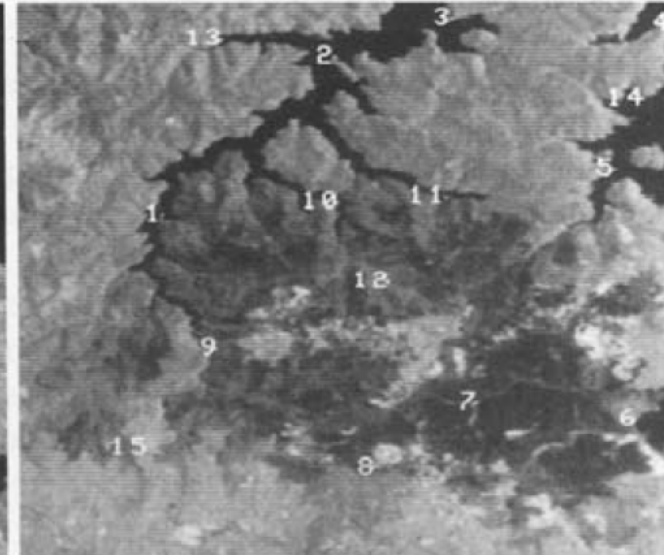
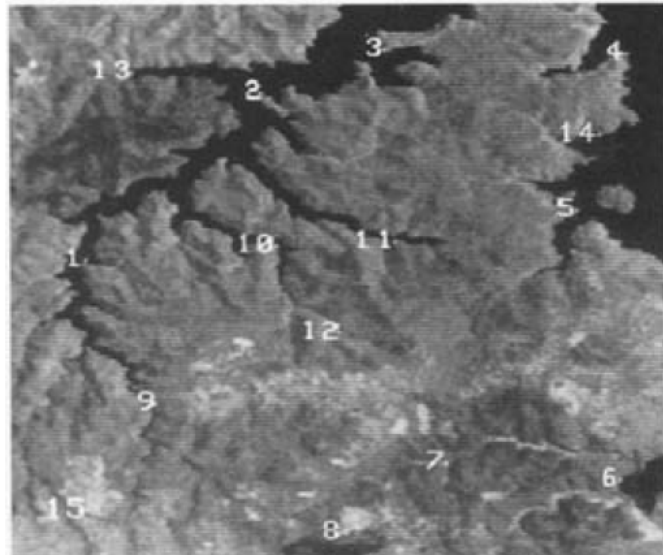
Example of Image to Image Registration (manual GCP selection - SSDA)

- We exemplify **image to image registration**, and more particularly
 - we see clearly the effect of control point distribution and
 - the significance of the order of the mapping polynomials to be used for registration
- Two *segments of Landsat MSS infrared image data* in the northern suburbs of Sydney were chosen:
 - one was acquired on December 29, 1979 and was used as the master;
 - the other was acquired on December 14, 1980 and was used as the slave image.
- **Two sets of control points** were chosen.
 1. In one the points were distributed as nearly as possible in a uniform manner around the edge of the image segment as shown in the following Figure (a), with some points located across the centre of the image.
 2. The second set of control points was chosen injudiciously, closely grouped around one particular region, to illustrate the resampling errors that can occur (see Figure (b)).
 - In both cases the control point pairs were co-located with the assistance of a sequential similarity detection algorithm (**correlation based**).
 - This worked well particularly for those control points around the coastal and river regions where the similarity between the images is unmistakable.
 - *Data curation hint!* To minimize tidal influences on the location of control points, those on water boundaries were chosen as near as possible to be on headlands, and certainly were never chosen at the ends of inlets.

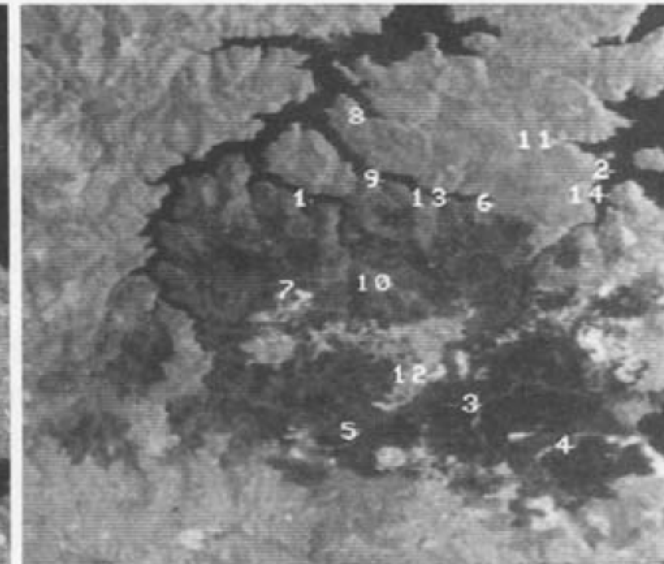
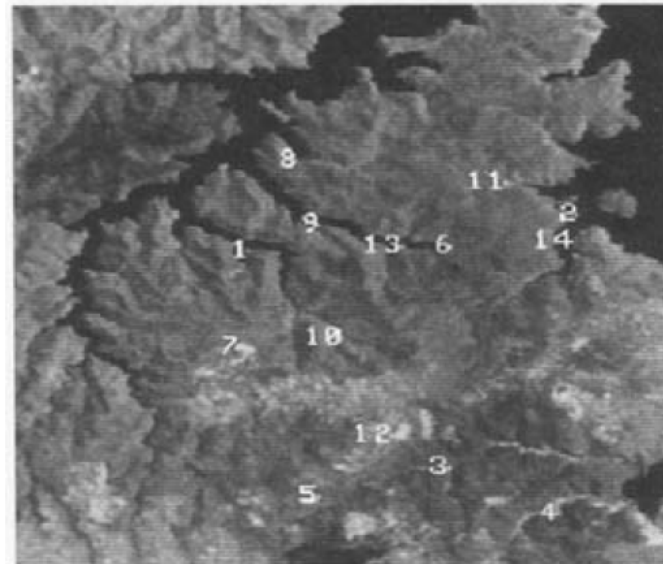
Example of Image to Image Registration (manual GCP selection - SSDA)

Ground Control Point selection

(a) Good
GCP set
distribution



(b) Poor
GCP set
distribution



a

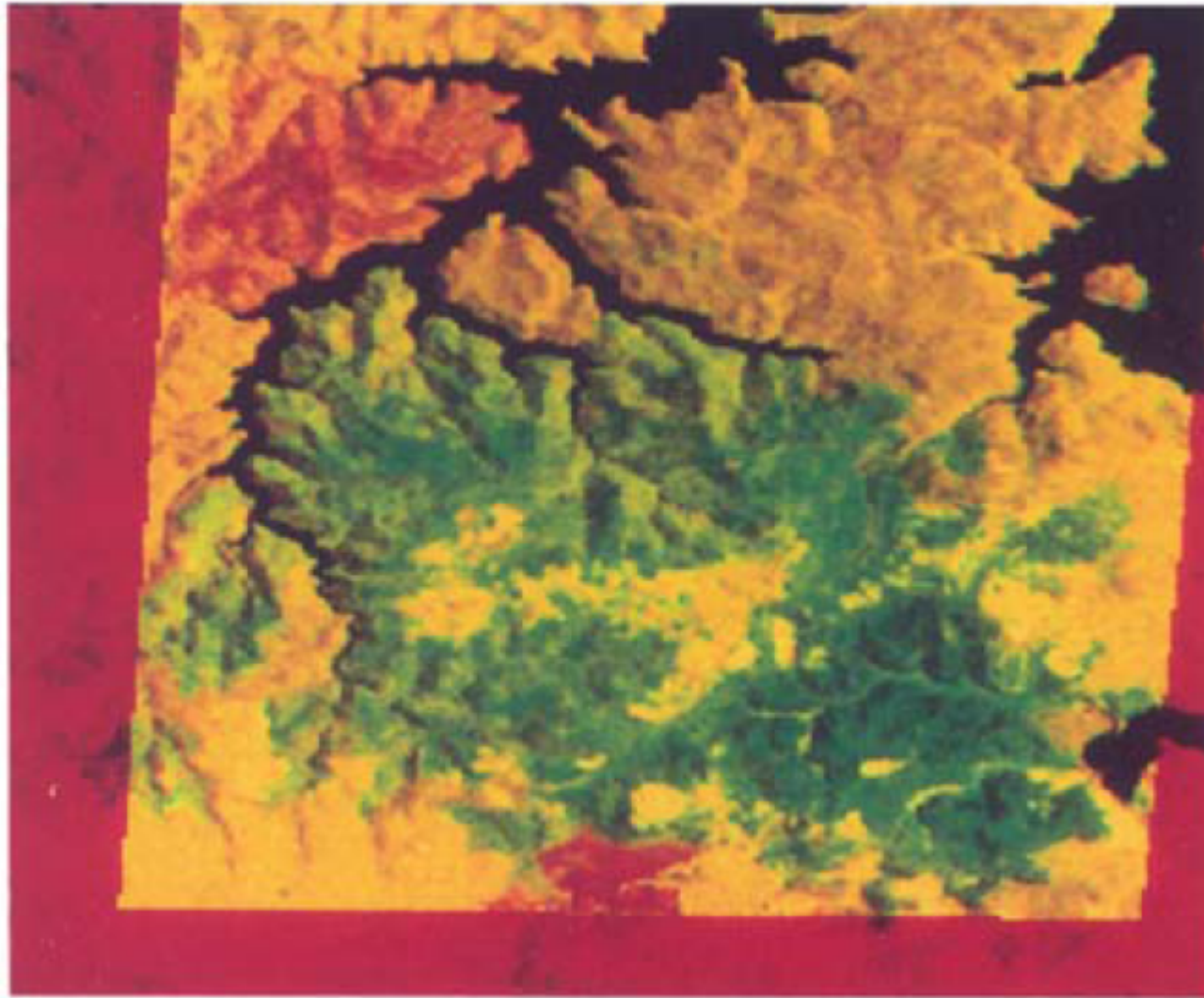
b

Examples of Image to Image Registration (manual GCP selection - SSDA)

- The adequacy of the **registration process** can be assessed visually if the master and resampled slave images can be **superimposed in different colors**.
 - The following figures show the master image in *red* with the resampled slave image superimposed in *green*.
 - Where **good registration** has been achieved the resultant is **yellow** (with the *exception* of regions of gross dissimilarity in pixel brightness – in this case associated with *fire burns*).
 - Misregistration shows quite graphically by a red-green separation.
- For both sets of control points ***third degree mapping polynomials*** were used along with ***cubic convolution resampling***.
 - As expected the first set of points led to an acceptable registration of the images (Figure a) whereas the second set gave a good registration in the immediate neighborhood of the points but beyond them produced gross distortion (Figure b), which is particularly noticeable (red-green separation) when the poor extrapolation obtained with third order mapping is demonstrated.
- The registration using the poor set of control points was repeated, this time only ***first order mapping polynomials*** were used.
 - While these obviously *will not remove non-linear differences between the images* and will give poorer matches at the control points themselves, they are well behaved in extrapolation beyond the vicinity of the control points and lead to an *acceptable registration*, as shown in Figure c.

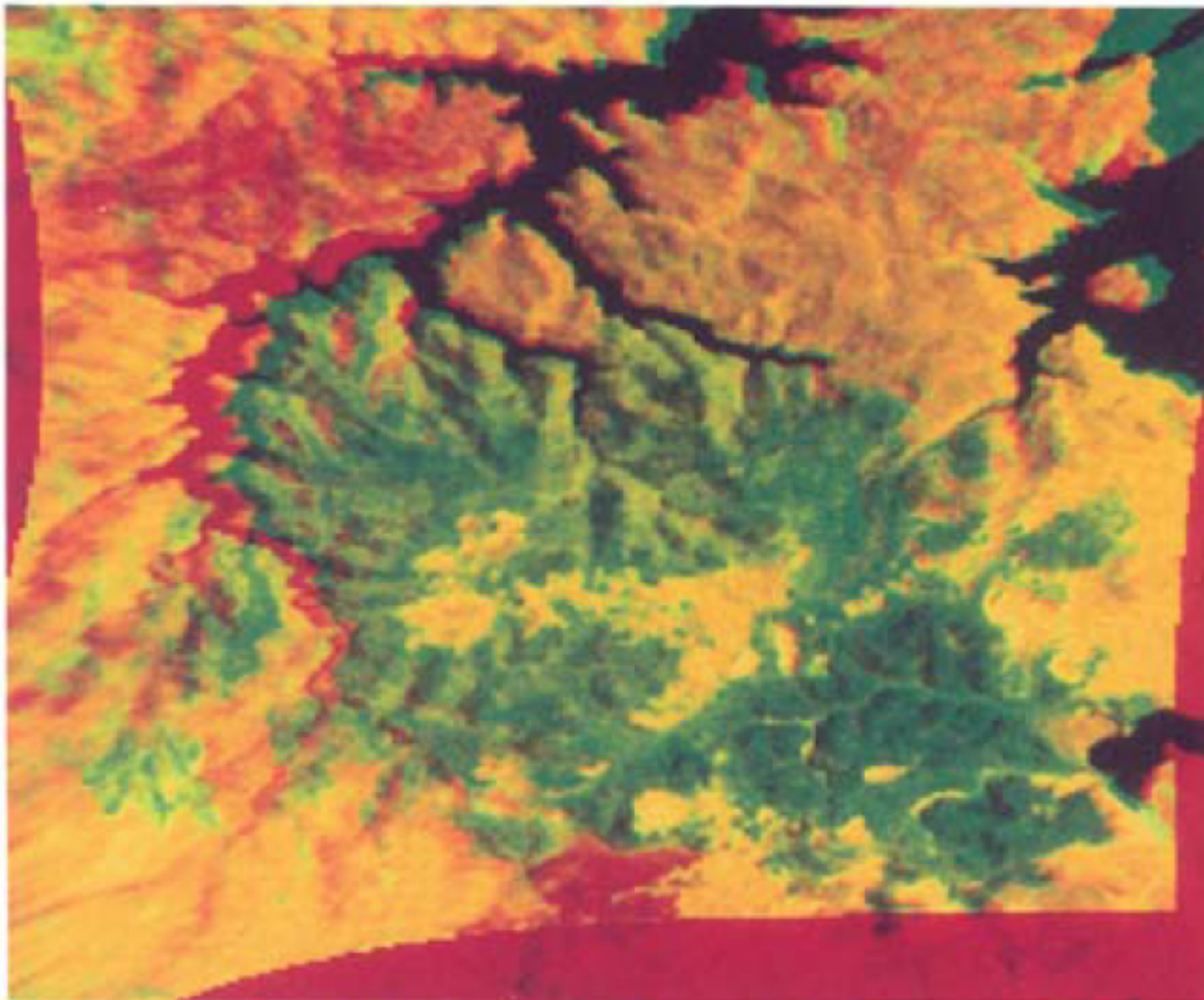
Example of Image to Image Registration (manual GCP selection - SSDA)

- Good GCP set – third degree mapping polynomials



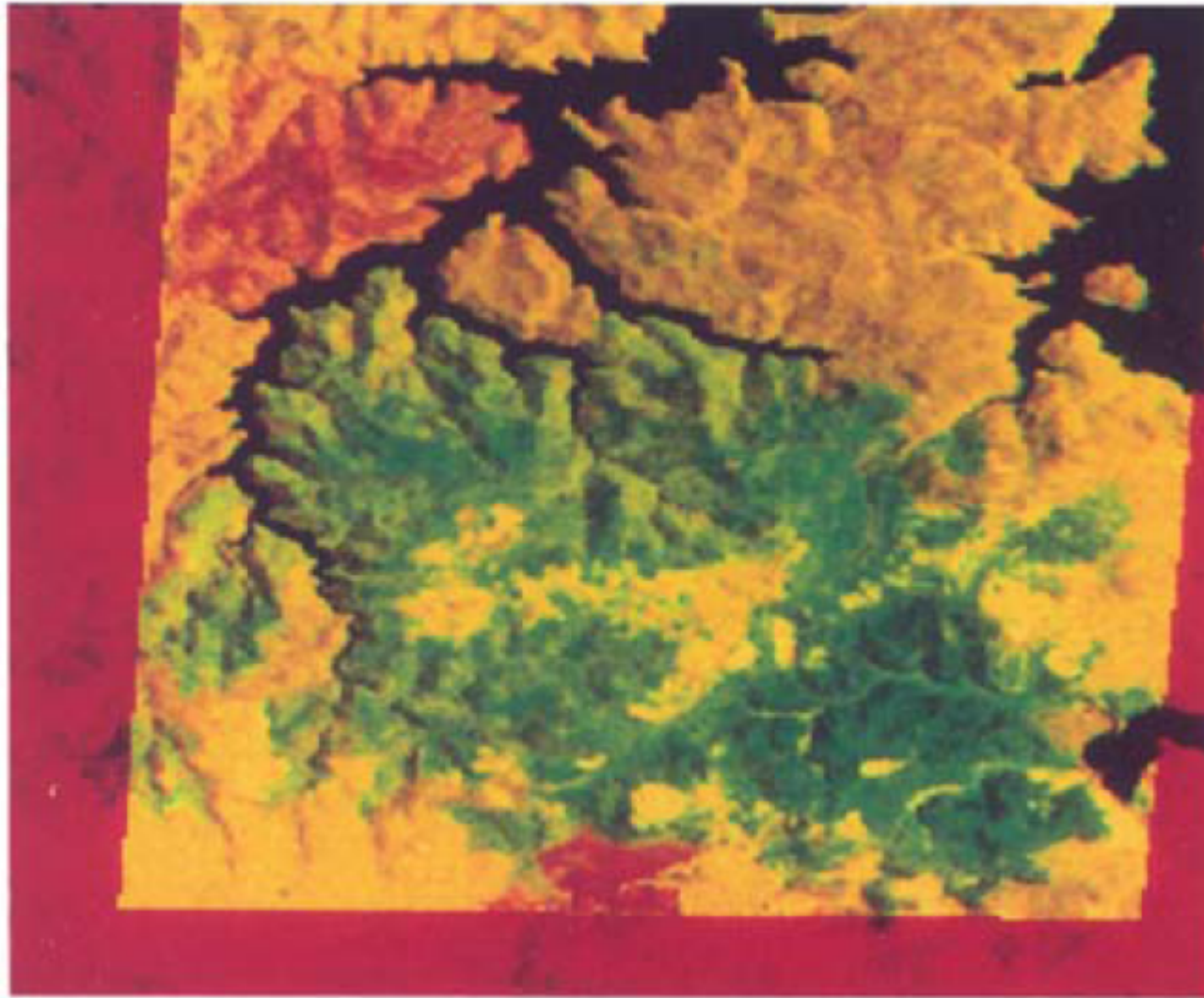
Example of Image to Image Registration (manual GCP selection - SSDA)

- Poor GCP set – third degree mapping polynomials



Example of Image to Image Registration (manual GCP selection - SSDA)

- Good GCP set – third degree mapping polynomials



Example of Image to Image Registration (manual GCP selection - SSDA)

- Poor GCP set – first degree mapping polynomials

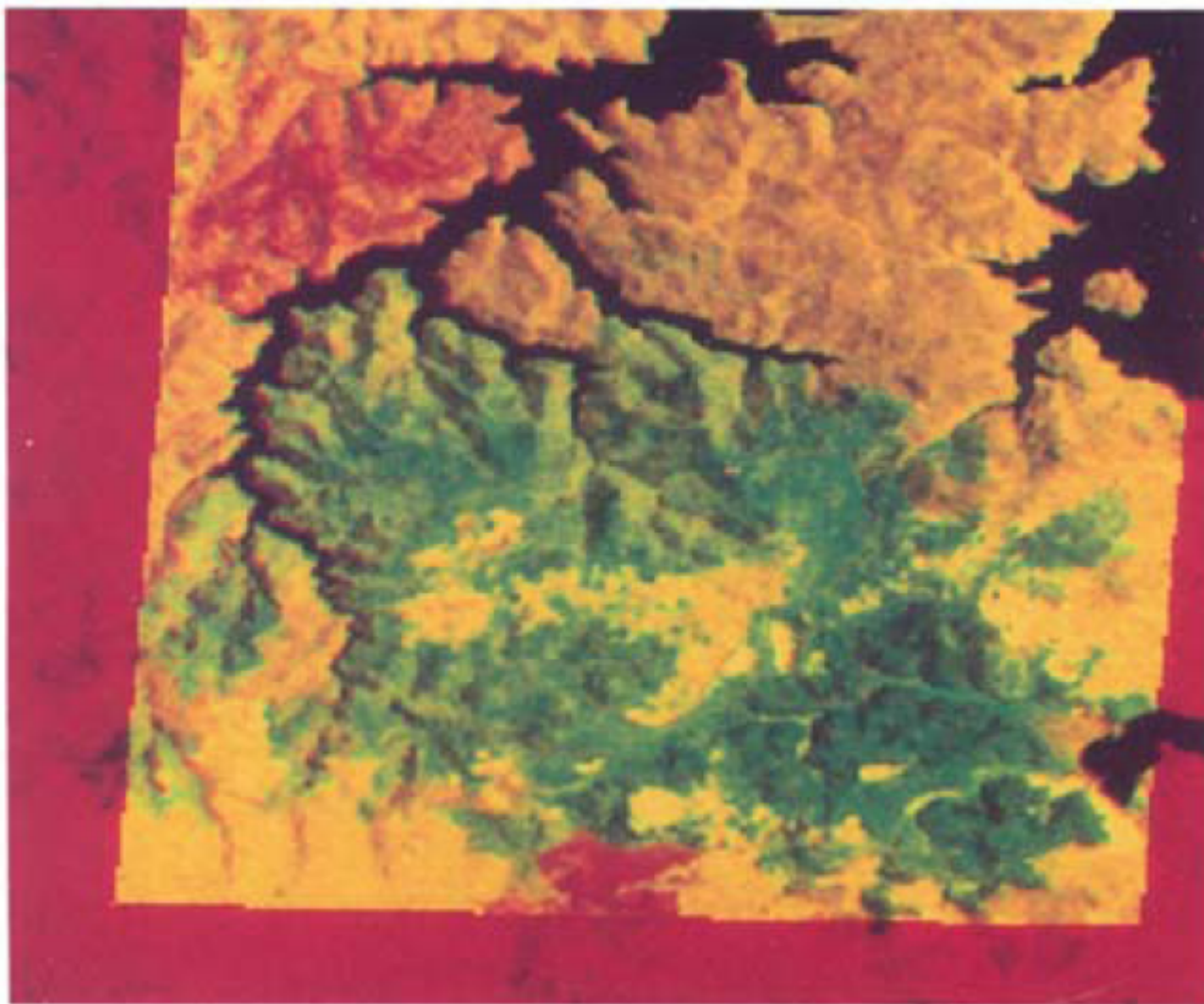


Image-to-image (affine) registration in frequency domain

Consider two $c \times c$ grayscale images, $g_1(i, j)$ and $g_2(i, j)$, where g_2 is offset relative to g_1 by an integer number of pixels:

$$g_2(i, j) = g_1(i', j') = g_1(i - i_0, j - j_0).$$

Taking the Fourier transform, we have

$$\hat{g}_2(k, \ell) = \frac{1}{c^2} \sum_{ij} g_1(i - i_0, j - j_0) e^{-i2\pi(ik+j\ell)/c},$$

or, with a change of indices to $i'j'$,

$$\begin{aligned}\hat{g}_2(k, \ell) &= \frac{1}{c^2} \sum_{i'j'} g_1(i', j') e^{-i2\pi(i'k+j'\ell)/c} e^{-i2\pi(i_0k+j_0\ell)/c} \\ &= \hat{g}_1(k, \ell) e^{-i2\pi(i_0k+j_0\ell)/c}.\end{aligned}$$

We find the 2D-translation by the **inverse transform of the cross-power spectrum** which exhibits a spike (delta) at coordinates (i_0, j_0) . Similar procedures are possible for rotation and scale variations (affine registration). Subpixel registration are also possible with refined methods.

Fourier translation property



Therefore, we can write

$$\hat{g}_2(k, \ell) \hat{g}_1^*(k, \ell) = |\hat{g}_1(k, \ell)|^2 e^{-i2\pi(i_0k+j_0\ell)/c},$$

where \hat{g}_1^* is the complex conjugate of \hat{g}_1 , and hence

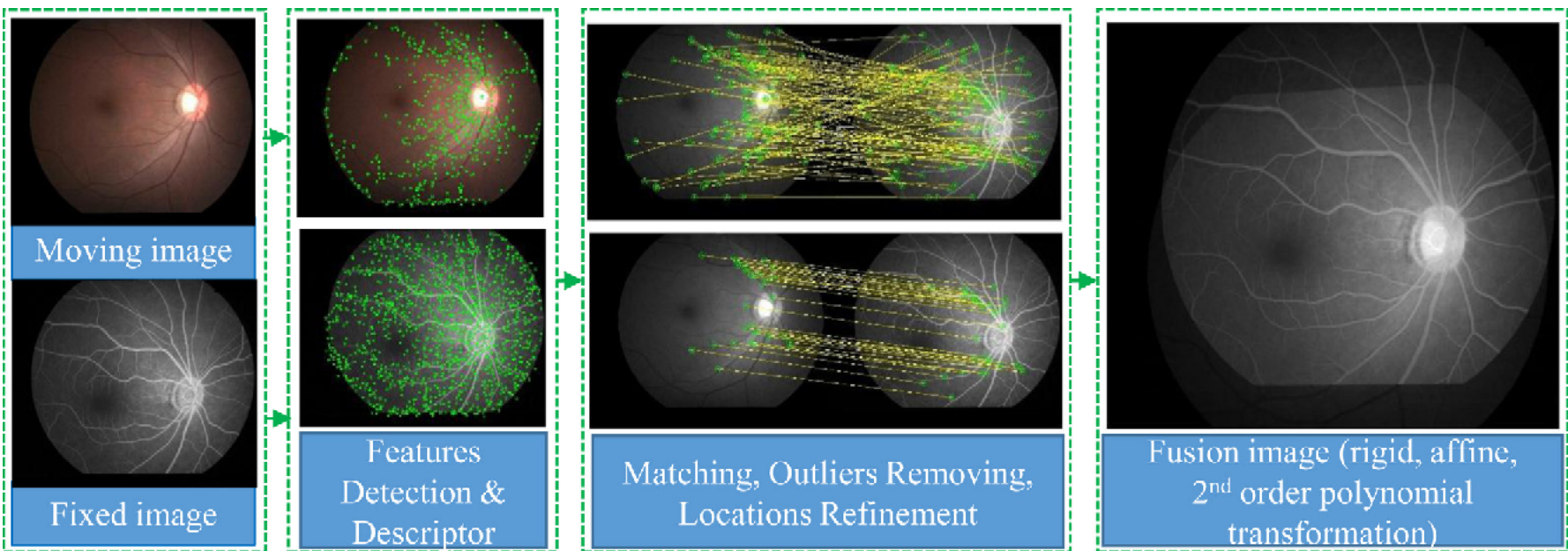
$$\frac{\hat{g}_2(k, \ell) \hat{g}_1^*(k, \ell)}{|\hat{g}_2(k, \ell) \hat{g}_1^*(k, \ell)|} = e^{-i2\pi(i_0k+j_0\ell)/c}.$$



Cross-power spectrum

Control Point Localisation by automated Feature Extraction and Matching

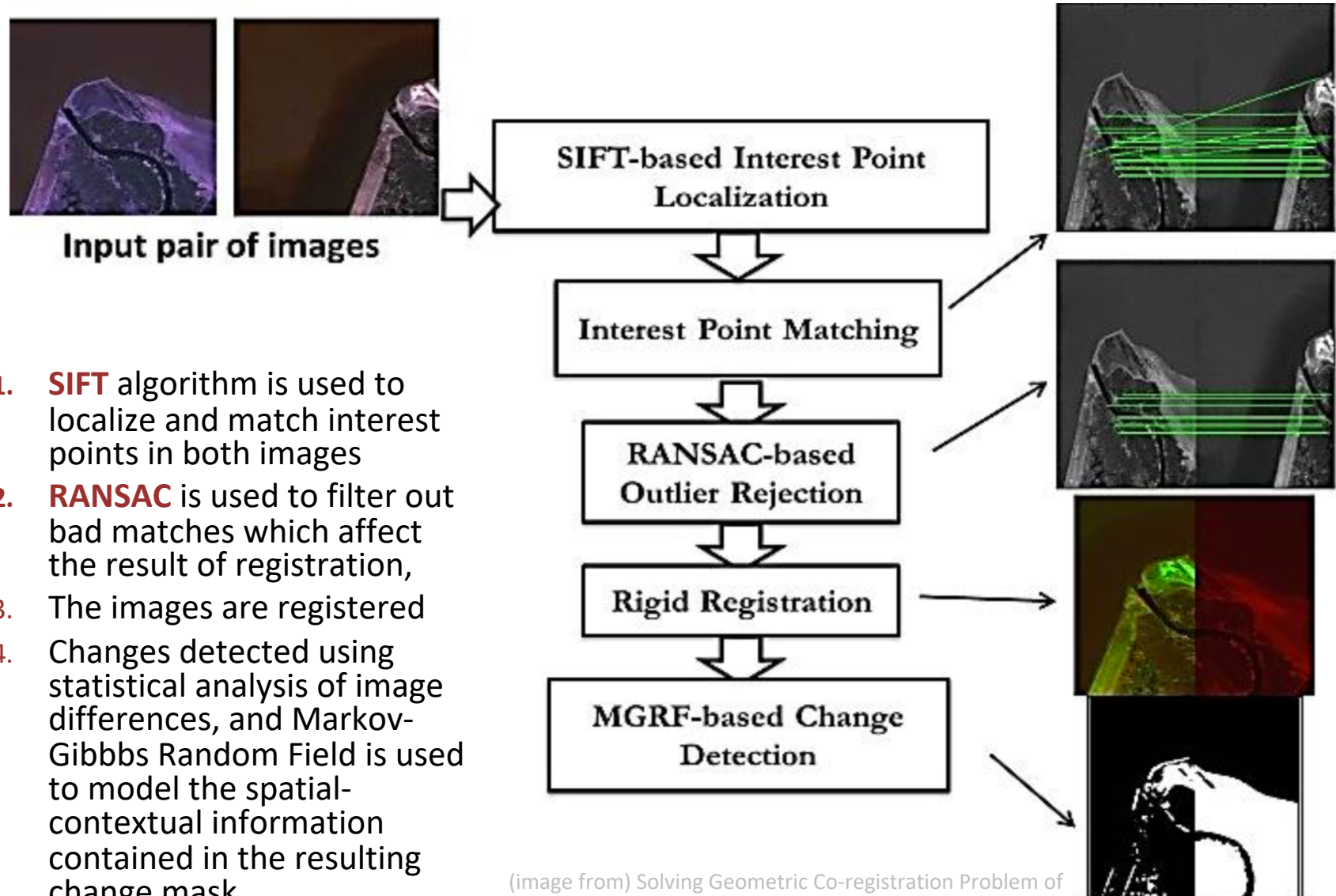
- Modern **feature based methods** can lead to more automated GCP localization both in the slave and master images, to produce more effective image to image registrations
 - Rotation, translation (and possibly scale) *invariant feature* search must be considered to be robust to geometric distortions
 - Feature sets are extracted from both the master and the slave images (or map and image)
 - Each feature is described by its geometric (geographic in the case of a map) position and an associated *signature*, i.e. a discriminative vector computed on the feature neighborhood.
 - **Correspondences** (matching) between couples of features in the master and slave images can be defined. Their potential number (combination) is very high but only a few are correct.
 - Registration transform is defined upon reliable feature correspondences.



Control Point Localisation by automated Feature Extraction and Matching

- Modern **feature based methods** can lead to more automated GCP localization both in the slave and master images, to produce more effective image to image registrations
 - Rotation, translation (and possibly scale) *invariant feature* search must be considered to be robust to geometric distortions
 - Feature sets are extracted from both the master and the slave images (or map and image)
 - Each feature is described by its geometric (geographic in the case of a map) position and an associated **signature**, i.e. a discriminative vector computed on the feature neighborhood.
 - **Correspondences** (matching) between couples of features in the master and slave images can be defined. Their potential number (combination) is very high but only a few are correct.
 - Registration transform is defined upon reliable feature correspondences (after outlier removal).
- Correspondence test procedures (feature matching + outlier removal) are of critical importance in order to determine, in a reliable and robust way, a set of correct correspondences which in turn define the associated set of ground control points.
- Various correspondence test approaches can be envisaged
 - Brute force methods (e.g. **RANSAC** technique, Fisher&Bolles 1981), based on feature point positions
 - **Feature description** methods (e.g. based on SIFT), based on signature similarity measures
 - *Mixed approaches*: for example, correspondences are first ranked and then skimmed based on signature similarity and then validated through tests based on geometric constraints (or viceversa) – or **correspondences are initially estimated by feature similarity measures and then consensus based statistical analysis (RANSAC) is used to reject outliers and estimate registration transform** (see example below).

Example of Image to Image Registration (automated feature based)



1. **SIFT** algorithm is used to localize and match interest points in both images
2. **RANSAC** is used to filter out bad matches which affect the result of registration,
3. The images are registered
4. Changes detected using statistical analysis of image differences, and Markov-Gibbs Random Field is used to model the spatial-contextual information contained in the resulting change mask

(image from) Solving Geometric Co-registration Problem of Multi-spectral Remote Sensing Imagery Using SIFT-Based Features toward Precise Change Detection – ISVC 2011